

Morphology of the pterothoracic musculature in Paraneoptera and its phylogenetic implication (Insecta: Neoptera)

Azuma Kawata 1 | Naoki Ogawa 2 | Kazunori Yoshizawa 1*

1. Systematic Entomology, School of Agriculture, Hokkaido University, Sapporo, 060-8589
Japan

2. Laboratory of Entomology, Tokyo University of Agriculture, Atsugi, Kanagawa, 243-0034
Japan

*corresponding author: psocid@agr.hokudai.ac.jp

Abstract

Although the monophyly of Paraneoptera (= hemipteroid orders or Acercaria, composed of Psocodea, Thysanoptera and Hemiptera) has been widely accepted morphologically, the results from molecular phylogenetic and phylogenomic analyses contradict this hypothesis. In particular, phylogenomic analyses provide strong bootstrap support for the sister group relationship between Psocodea and Holometabola, i.e., paraphyly of Paraneoptera. Here, we examined the pterothoracic musculature of Paraneoptera, as well as a wide range of other neopterous insect orders, and analysed its phylogenetic implication. By using the synchrotron microcomputed tomography (μ CT) and parsimony-based ancestral state reconstruction, several apomorphic conditions suggesting the monophyly of Paraneoptera, such as the absence of the **II/IIItpm7**, **IIscm3**, **IIIspm2** and **IIIscm3** muscles, were identified. In contrast, no characters supporting Psocodea + Holometabola were recovered from the thoracic muscles. These results provide additional support for the monophyly of Paraneoptera, together with the previously detected morphological apomorphies of the head, wing base, and abdomen.

Keywords: Hemiptera, Holometabola, Psocodea, Thysanoptera, μ CT

1 | INTRODUCTION

Recent phylogenomic studies have provided robust backbone trees for the higher systematics of insects (e.g., Niehuis et al., 2012; Misof et al., 2014; Johnson et al., 2018; Wipfler et al., 2019). The results from the phylogenomic analyses are concordant with the traditional insect higher systematics in many respects (e.g., nonmonophyly of Entognatha: Machida, 2006; monophyly of Polyneoptera: Yoshizawa, 2011; higher-level phylogeny of Holometabola: Beutel et al., 2011). In contrast, there were a few apparent discordances between them. One of the most significant and surprising results was the nonmonophyly of Paraneoptera (= hemipteroid orders or Acercaria composed of Psocodea, Thysanoptera and Hemiptera; the latter two compose the superorder Condylgnatha) (Misof et al., 2014), i.e., Psocodea was placed as the sister taxon of Holometabola with a high bootstrap support value. In contrast, the monophyly of Paraneoptera has long and consistently been recognized with having a number of morphological apomorphies. Those include enlarged postclypeus and cibarial muscles, elongated lacinia detached from stipes, specialized wing base articulations, a single abdominal ganglionic complex, reduced number of Malpighian tubules, and reduced cerci (Hennig, 1981; Kristensen, 1991; Yoshizawa & Saigusa, 2001; Beutel et al., 2014; Wang et al., 2016; Yoshizawa & Lienhard, 2016).

The nonmonophyly of Paraneoptera was recovered and also received a high support value from a subsequent phylogenomic analysis with greatly expanded taxon and gene samplings (Johnson et al., 2018). However, it was also shown that the phylogenomic datasets contain apparently conflicting signals regarding the interordinal phylogeny of Paraneoptera, even though Psocodea + Holometabola received high bootstrap support from the concatenated datasets (Misof et al., 2014; Johnson et al., 2018). For example, four cluster likelihood mapping analyses (Strimmer & von Haeseler, 1997) showed that the phylogenomic datasets also contained signals supporting the monophyly of Paraneoptera, as well as signals for Psocodea + Holometabola or Condylgnatha + Holometabola (Misof et al., 2014; Johnson et al., 2018). In the polyneopteran phylogenomic analysis by Wipfler et al. (2019), limited paraneopteran samples were employed as outgroup taxa, and in the tree, Paraneoptera was recovered as a monophyletic group. This showed that phylogenetic relationships among Psocodea, Condylgnatha and Holometabola are also highly sensitive to taxon sampling. Therefore, further testing for such an unstable phylogenomic result is needed based on independent datasets.

The insect thorax contains many muscles that play important roles in insect locomotion (e.g., Snodgrass, 1935; Maki, 1938; Brodsky, 1994). Furthermore, most of the muscles can be

homologized throughout neopteran insects (Friedrich & Beutel, 2008, 2010). Such properties of insect thoracic muscles (i.e., many characteristics that can be homologized for a wide variety of insect orders) indicate their potential usefulness in estimating the higher-level phylogenetic relationships of insects. For example, our previous study showed that the thoracic musculature contains a clear signal for resolving the higher-level phylogeny of Psocodea (Kawata et al., 2022). However, this character system has not been utilized for testing the monophyly and phylogeny of Paraneoptera.

In this study, we examined the pterothoracic musculature of paraneopteran orders, as well as holometabolan insects, and tested the monophyly of Paraneoptera. We used the synchrotron microcomputed tomography (μ CT) to reconstruct the musculature of a wide variety of neopteran taxa (polyneopteran Plecoptera, paraneopteran Psocodea, Thysanoptera and Hemiptera and holometabolan Hymenoptera, Raphidioptera, Megaloptera, Mecoptera, Trichoptera and Lepidoptera). As a result, we identified four muscle reduction characters suggesting the monophyly of Paraneoptera. In contrast, there are no characters supporting Psocodea + Holometabola, the relationship suggested by phylogenomic studies. Although the phylogenetic value of reduction characters is generally regarded as low, the present results provide additional support for the monophyly of Paraneoptera.

2 | MATERIALS AND METHODS

The thoracic musculature of the fully winged species selected from major lineages of Paraneoptera and Holometabola (excluding orders lacking flight function on at least one pair of wings, such as Coleoptera, Strepsiptera, Siphonaptera or Diptera) were examined. Multiple species representing different suborders were selected from each paraneopteran order, and a single not highly specialized species was selected from each holometabolan order. Auchenorrhyncha species were not included in the analyses due to the significant modification of their hind thorax associated with their jumping behavior (Ogawa & Yoshizawa, 2017). Fully winged form of Coleorrhyncha was not available for the study. A polyneopteran taxa, Plecoptera, was also examined. The species included in the analyses are listed in Table 1. Samples were either fixed with 80% ethanol or FAA solution (formalin:alcohol:acetic acid = 6:16:1) and then preserved in 80% ethanol. Samples were dehydrated with 80–100% ethanol in ascending order before critical point drying (EM CPD300, Leica, Wetzlar, Germany) to remove water without serious organ shrinkage. Samples were then scanned using synchrotron μ CT at the BL47XU, BL20B or BL20XU (Uesugi et al., 2012) beamlines of the Super Photon ring-8 GeV (SPring-8; Hyogo, Japan)

using a stable beam energy at 8 keV (for BL47XU and BL20B) or 15 keV (for BL20XU) in absorption-contrast mode. The tomography system consisted of a full-field X-ray microscope with Fresnel zone plate optics (Uesugi et al., 2017). We used semiautomatic segmentation algorithms based on grey-value differences in ITK-SNAP 3.6 software (Yushkevich et al., 2006) to obtain 3D representations of the thoracic musculature.

Based on the presence/absence of each pterothoracic muscle (Table 2), a data matrix was constructed (Online Supplement). Several muscle pairs (**II/III_{dvm}2** and **3**, **II/III_{pcm}2** and **3**, and **II_{vlm}3** and **5**) were coded together as a single character for the following reasons: When two muscles were observed, their homology identification was straightforward. However, when one of these muscles was absent, the homology of the remaining muscle was impossible to identify because of the shared origination and insertion sites (in the case of **II_{vlm}**, the origination site, i.e., the furca for **II_{vlm}3** and spina for **II_{vlm}5**, was different, but the furca and spina were fused in paraneopteran taxa; thus, distinction of these muscles was impossible when one of them was absent). Using the data matrix, the parsimonious character mapping analyses were conducted to uncover the phylogenetic signal contained in the pterothoracic musculature. The polyneopteran order Zoraptera and the mecopteran family Nannochoristidae were also included in the character mapping analyses, and data of these taxa were selected from the μ CT-based study by Friedrich & Beutel (2008) and Friedrich & Beutel (2010), respectively. We compared results from the character mapping based on two alternative trees, supporting the monophyly of Paraneoptera (as suggested morphologically) vs. supporting the Psocodea + Holometabola (nonmonophyly of Paraneoptera: as suggested from phylogenomics). Other topologies (i.e., monophyly of Polyneoptera, Condylgnatha, Holometabola, and each insect order, and phylogeny of holometabolan orders) were fixed according to Misof et al. (2014). The parsimonious mapping of character changes was conducted using Mesquite 3.81 (Maddison & Maddison, 2023) and MacClade 4.08 (Maddison & Maddison, 2001).

3 | RESULTS

Pterothoracic musculature of paraneopteran taxa (Figs 1-5)

The paraneopteran pterothoracic muscles recovered by the present examinations were homologized and listed according to Friedrich & Beutel (2008, 2010). Muscles not detected in the present examinations were not listed. See Table 2 and Online Supplement for the condition of holometabolan and polyneopteran taxa. Homology interpretation for some muscles is argued in the Discussion chapter.

3.1 | Mesothorax

3.1.1 | Dorsal Longitudinal Muscles

IIdlm1 is the largest mesothoracic muscle originating from large area of the anterior lobe of mesoscutum and inserting into the center of mesophragma (Figs 1–5). Usually, it consists of multiple bundles, which are sometimes recognized as distinct muscles (Table 2). In Heteroptera, this muscle extends over the metanotum following the posterior extension of the mesoscutellum (Fig. 5A).

IIdlm2 is a thick muscle originating from the posteromedial part of mesonotum and inserting into the mesophragma, lateral to the insertion point of **IIdlm1** (Figs 1–5). It usually consists of two bundles, which are sometimes recognised as distinct muscles (Table 2). **IIdlm2** is absent in Terebrantia (Thysanoptera) (Fig. 3A)

3.1.2 | Dorsoventral Muscles

IIdvm1 is (when present) a long and thick muscle originating from the anterior region of the lateral lobe of mesoscutum and inserting into the precoxal bridge. However, in Sternorrhyncha, it originates from the posterior region of the lateral mesoscutal lobe. It frequently consists of multiple bundles, which are recognized as distinct muscles sometimes (Table 2). This muscle is about the same in size as (Troctomorpha: Psocodea) or larger than (Psocomorpha: Psocodea, Thysanoptera, Hemiptera) **IIdvm2**. However, it is absent in Troctomorpha (Psocodea), and probably due to this modification, **IIIdvm2** is strongly developed in this taxon.

IIdvm2/3 is a long muscle originating from the anterior region of the lateral lobe of mesoscutum and inserting into trochantin. It is particularly thin in Psocomorpha (Psocodea) (Kawata et al., 2022) and Sternorrhyncha (Hemiptera) (Fig. 4B), and is absent in Thysanoptera (Fig. 3A).

IIdvm4 is a twisted thick and long muscle originating from the posterior region of the lateral lobe of mesoscutum, posterior to lateral margin of the origination site of **IIdlm2**, and inserting into the posterior mesocoxal rim. However, in Sternorrhyncha, it originates from the anterior region of the lateral mesoscutal lobe. It usually consists of two bundles and is dorsally flattened, which are sometimes considered to be distinct muscles (Table 2). It is usually arranged

vertically, but in Heteroptera, it is arranged diagonally (Fig. 5B) and is absent in Thysanoptera (Fig. 3).

IIdvm5 is the thinnest among the mesothoracic dvm muscles originating from the posterior region of the lateral lobe of mesoscutum and inserting into the posterior mesocoxal rim (an exact insertion point was not clearly observable in some species) (Figs 1–5). It is absent in Thysanoptera (Fig. 3).

IIdvm6 is a twisted thick and long muscle originating from the subalare and inserting into the posterior mesocoxal rim, lateral to the insertion site of **IIdvm4** (Figs 1–3). This muscle is composed of two bundles but is absent in Hemiptera (Figs 4–5).

IIdvm7 is a long and thick muscle originating from the middle of the lateral lobe of the mesoscutum, posterior to the origination site of **IIdvm1/2** and inserting into the trochanter via a tendon. This muscle consists of three bundles but is absent in Thysanoptera (Fig. 3) and Sternorrhyncha (Hemiptera) (Fig. 4).

IIdvm8 is a muscle originating from the anterolateral part of the furca and inserting into the ventrolateral part of phragma. It is generally short and thin, but in Thysanoptera (Fig. 3A) and Heteroptera (Hemiptera) (Fig. 5A), it is thick and is absent in Psocodea (Fig. 2).

3.1.3 | Pleural Muscles

IItpm1 is a small muscle originating from the base of prealar arm and inserting into the anterodorsal edge of the anepisternum. Usually, the insertion point of this muscle is located below its origination point. However, due to the dorsal extension of the pleural sclerites, its insertion point is positioned above the origination point in Heteroptera (Hemiptera) (Fig. 5C).

IItpm2 is a small muscle originating from the base of prealar arm, anterior to the origination site of **IItpm1**, and inserting into the base of the pleural wing process. This muscle usually runs horizontally, but in Heteroptera (Hemiptera), it runs almost vertically due to the dorsal extension of the pleural sclerites (Fig. 5C).

IItpm3 is absent in all paraneopteran taxa.

IItpm4 is absent in all paraneopteran taxa.

IItpm5 is a flattened muscle originating from the pleural arm and inserting into the median part of the notal margin. Usually, the insertion point of this muscle is located anterior to its origination point (Figs 1C, 2C, 4C), but in Thysanoptera, the insertion point is located posterior to the origination point due to the reduced

size of the notum (Fig. 3A). This muscle is absent in Heteroptera (Hemiptera) (Fig. 5).

IItpm6 is absent in all paraneopteran taxa.

IItpm7 is a rather well developed muscle originating from the dorsal region of the anepisternum and inserting into the 3rd axillary sclerite. Among the paraneopteran taxa, this muscle is only detected in Heteroptera (Hemiptera) (Fig. 5C).

IItpm9 is a rather well developed, fan-shaped muscle broadly expanded anteroventrally, originating from the pleural arm, posterodorsal to the origination site of **IItpm4**, and inserting into the anterior arm of the 3rd axillary sclerite. This muscle is absent in Thysanoptera (Fig. 3) and Hemiptera (Figs 4–5).

IItpm10 is a muscle originating from the posterior region of the epimeron and inserting into the subalare. Generally, the origination site of this muscle is located above its insertion point, but in Sternorrhyncha (Hemiptera), it is shifted ventrally, resulting in the elongation and vertical arrangement of the muscle (Fig. 4C). This muscle is absent in Psocodea (Fig. 3) and Heteroptera (Hemiptera) (Fig. 5).

IItpm11 is only observed in Sternorrhyncha (Hemiptera) among the taxa examined here. It originates from the pleural arm and inserts into the subalare, just anterior to the insertion point of **IItpm10** (Fig. 4C). It somewhat resembles **IItpm9** of Psocodea (Fig. 2C), but judging from its insertion point, the present interpretation is supported.

IItpm2 is absent in all paraneopteran taxa.

IItpm1 is a thick muscle originating from the dorsal part of the anepisternum, including the anterior part of the basalare, and inserting into the lateral region of the precoxal bridge, lateral to the insertion site of **IIdvm1**. It sometimes consists of multiple bundles, as seen in Thysanoptera (Fig. 3B) and Heteroptera (Hemiptera) (Fig. 5B). It is absent in Troctomorpha and Psocomorpha (Psocodea) (Kawata et al., 2022).

IItpm2 is a long but very thin muscle originating from the tip of the mesofurcal arm and inserting into the mesopleural arm, ventral to the origination site of **IItpm9**. It is absent in Troctomorpha, Psocomorpha (Psocodea) (Kawata et al., 2022) and Sternorrhyncha (Hemiptera) (Fig. 4).

IItpm4 is absent in all paraneopteran taxa.

IIspm6 is a muscle originating from the tip of the mesofurcal arm, posterointernal to the origination point of **IIspm2**, and inserting into the anterior margin of the metanepisternum. It is highly variable in shape: very thin and long, arranged vertically in Psocodea (Fig. 2C); much thicker and long, arranged vertically in Thysanoptera (Fig. 3B); thick and short, arranged vertically in Sternorrhyncha (Fig. 4C); and flattened and fan-shaped, arranged horizontally in Heteroptera (Fig. 5B).

IIpcm1 is a muscle originating from the anterior part of the anepisternum and inserting into the trochantin. It presents in Psocodea (Fig. 2C) and Terebrantia (Thysanoptera) (Fig. 3C), and is absent in other paraneopteran taxa. The condition observed in Psocodea well matches to the definition of this muscle (Fig. 2C), but in Terebrantia, the muscle originates from the mid-part of the anepisternum (Fig. 3C), probably due to the expansion of the precoxal area in Thysanoptera.

IIpcm2 is a thick muscle originating from the basalare, posterior to the origination site of **IIspm1**, and inserting into the anterior mesocoxal rim. It usually runs vertically and broadens ventrally, but in Heteroptera, it runs horizontally (Fig. 5C) according to the posterior positioning of the mesocoxa. It is absent in Thysanoptera (Fig. 3).

IIpcm3 is a thick muscle running parallel with **IIpcm2**, originating from the basalare, posterior to the origination site of **IIpcm2**, and inserting into the anterolateral mesocoxal rim, posterior to the insertion site of **IIpcm2**. It is absent in Thysanoptera (Fig. 3: see also Materials and Methods for interpretation).

IIpcm4 is a muscle originating from the ventral region of the anepisternum and inserting into the anterolateral coxal rim. Within the Paraneoptera, this muscle is only detected in Thysanoptera (Fig. 3B).

IIpcm5 is a thick and long muscle composed of two bundles. It originates from the basalare, lateral to the origination site of **IIspm1** and anterior to the origination site of **IIpcm2**, and inserts into the trochanter via a tendon. It is absent in Thysanoptera and Hemiptera.

IIpcm6 is a thick and long muscle originating from the pleural arm, just ventral to the insertion site of **IIspm2**, and inserting into the trochanter via a tendon. It presents only in Heteroptera (Fig. 5B) among the presently examined taxa.

3.1.4 | Sternal Muscles

IIvIm3 is a muscle originating from the posteroventral margin of the mesothoracic furcal arm and inserting into the anterior tip of the metathoracic furca. It is generally long (Figs 3–5), but due to the posterior extension of the mesofurcal arm and the anterior extension of metafurcal arm, this muscle is extremely short in Psocodea (Fig. 2D). It is absent in Tublifera (Thysanoptera) (Online Supplement).

IIscm1 is a small muscle originating from the precoxal sternal region and inserting into the anterior coxal rim. It is absent in Psocodea (Fig. 2).

IIscm2 is a flattened muscle originating from the ventrolateral side of the base of the mesofurcal arm and inserting into the posterior mesocoxal rim, close to the insertion site of **IIsvm4**. It consists of multiple bundles in Psocodea (Fig. 2C) and Heteroptera (Fig. 5E).

IIscm3 is a muscle originating from the ventral part of the furcal arm and inserting into the mesal coxal rim. It only presents in Terebrantia (Thysanoptera) among the presently examined paraneopteran taxa, in which this muscle is rather well developed among the scm muscles (Fig. 3D).

IIscm4 is a long but thin, flattened muscle originating from the tip of the mesofurcal arm, ventral to the origination point of **IIspm2**, and inserting into the lateral mesocoxal rim close to its articulation point. It is absent in Hemiptera (Figs 4–5).

IIscm6 is a flat muscle originating from the dorsolateral part of mesofurca, ventrolateral to the insertion point of **IvIm7**, and inserting into the trochanter via a tendon, mesal to the insertion site of **IIsvm7**. It usually consists of two bundles (Figs 2, 3, 5) but of a single bundle in Sternorrhyncha (Hemiptera) (Fig. 4C, E).

IIscm7 is a thin, flattened muscle originating from the posteroventral surface of the mesofurcal arm, ventral to the origination site of **IIvIm3**, and inserting into the anterior metacoxal rim. It presents in Psocodea (Fig. 2D) and Terebrantia (Thysanoptera) (Fig. 3A) among the presently examined taxa, and in the latter taxon, this muscle is very long, according to the expanded precoxal region of the metathorax.

3.2 | Metathorax

3.2.1 | Dorsal Longitudinal Muscles

IIIdIm1 is a large muscle originating from the near center of the mesophragma and inserting

into the metaphragma. It usually consists of 4 or 5 bundles, which were sometimes recognized as distinct muscles (Table 2). This is one of the principal indirect flight muscles but is absent in Hemiptera (Figs 4A, 5A).

IIIIdlm2 is a thick muscle originating from the central part of the lateral lobe of the metascutum and inserting into the metaphragma, lateral to the insertion site of **IIIIdlm1**. It usually consists of multiple bundles, which were sometimes recognized as distinct muscles (Table 2). **IIIIdlm2** usually runs diagonally, but in Thysanoptera, it runs almost horizontally, parallel to **IIIIdlm1** (Fig. 3A). This muscle is absent in Heteroptera (Fig. 5A).

3.2.2 | Dorsoventral Muscles

IIIIdvm1 is large long muscle originating from the anterolateral region of the scutum and inserting into the precoxal bridge. It usually consists of multiple bundles, which were recognized as distinct muscles sometimes (Table 2). Due to the absence of the metathoracic precoxal bridge, this muscle is absent in Psocodea (Fig. 2A).

IIIIdvm2/3 is a thick and long muscle originating from the anteroventral part of the scutum and inserting into the trochantin. This muscle is usually smaller than **IIIIdvm1**, but **IIIIdvm2** is much larger than **IIIIdvm1** in Heteroptera (Fig. 5A). **IIIIdvm2/3** is absent in Troctomorpha (Psocodea) (Kawata et al., 2022), Thysanoptera (Fig. 3A) and Sternorrhyncha (Hemiptera) (Fig. 4A).

IIIIdvm4 is a thick and long muscle originating from the anterior part of the scutum and inserting into the posterior coxal margin. It usually consists of multiple bundles which were sometimes recognized as distinct muscles (Table 2). It is usually arranged vertically (Figs 1A), but due to the enlargement of coxa, it is arranged diagonally in Heteroptera (Fig. 5B). This muscle is absent in Trogiomorpha (Psocodea) (Fig. 2), Thysanoptera (Fig. 3) and Sternorrhyncha (Hemiptera) (Fig. 4).

IIIIdvm5 is a long muscle originating from the posterolateral region of the lateral lobe of the metanotum and inserting into the posterior metacoxal rim. It consists of one or two bundles, but their distinction is very obscure. It usually runs vertically (Fig. 2B), but due to the posterior shift of the metacoxa, this muscle runs much more horizontally in Thysanoptera (Fig. 3B).

IIIIdvm6 is a thick and long muscle originating from the subalare and inserting into the posterior metacoxal rim, very close to the insertion site of **IIIIdvm5**. It consists

of two twisted bundles. This muscle is absent in Terebrantia (Thysanoptera) (Fig. 3) and Heteroptera (Hemiptera) (Fig. 5).

III_dvm7 is a thickest metathoracic muscle (when present) originating from the median region of the lateral lobe of the metascutum, anterior to the origination site of **III_dvm5** and posterolateral to the origination site of **II_dvm2**, and inserting into the trochanter via a tendon, mesal to the origination site of **III_pcm5/6**. It consists of three bundles but is absent in Thysanoptera (Fig. 3).

III_dvm8 is a muscle originating from the posterolateral surface of the metafurcal arm, mesal to the origination site of **II_vlm3**, and inserting into the ventrolateral part of the metaphragma. It usually tapers toward the origination position and is arranged more or less horizontally (Figs 1A, 2A and 4C). However, in Thysanoptera and Heteroptera, this muscle inserts into the more dorsal region of the metaphragma (Figs 3A, 5A) and thus is arranged more vertically.

3.2.3 | Pleural Muscles

III_tpm1 is a small muscle originating from the mesophragma and inserting into the basalare. It is absent in Thysanoptera (Fig. 3E).

III_tpm2 is a small, fan-shaped muscle originating from the base of the prealar sclerite and inserting into the pleural arm. This is absent in Heteroptera (Fig. 5B).

III_tpm3 is a small muscle originating from the anterolateral region of the metanotum and inserting into the basalare. Among the taxa examined here, it is only observed in Trogiomorpha (Psocodea) (Fig. 2E).

III_tpm4 is a small muscle originating from the pleural arm, next to the insertion point of **III_tpm2**, and inserting into the proximal margin of the 1st axillary sclerite. It only presents in Thysanoptera among the presently observed paraneopteran taxa (Fig. 3C).

III_tpm5 is a small, flattened muscle originating from the pleural arm and inserting into the middle of the lateral notal margin. It is absent in Terebrantia (Thysanoptera) (Fig. 3) and Heteroptera (Fig. 4).

III_tpm6 is absent in all paraneopteran taxa examined.

III_tpm7 is absent in all paraneopteran taxa examined.

III_tpm9 is a relatively large muscle (among the tpm muscles) originating from the pleural arm, next to the origination site of **III_tpm4**, and inserting into the anterior arm of the 3rd axillary sclerite. It is absent in condylognathan taxa (Figs 3–5).

IIItpm10 is a narrow but elongated muscle originating from the posterodorsal region of the epimeron and inserting into the subalare. Among the paraneopteran taxa examined, it only presents in Thysanoptera (Fig. 3C).

IIItpm11 is a small muscle originating from the pleural ridge close to the pleural arm and inserting into the subalare. Among the paraneopteran taxa examined, it only presents in Sternorrhyncha (Hemiptera) (Fig. 4C).

IIIppm1 is absent in all paraneopteran taxa examined.

IIIppm2 is absent in all paraneopteran taxa examined.

IIIspm1 is, when present, a thick muscle originating from the basalare and inserting into the precoxal region. It is especially enlarged in Thysanoptera (Fig. 3B) due to the expansion of the precoxal area. This muscle is absent in Psocodea (Fig. 2) and Heteroptera (Fig. 5).

IIIspm2 is absent in all paraneopteran taxa examined.

IIIpcm1 is a fan-shaped muscle tapering ventrally, originating from the dorsal part of the anepisternum and inserting into the trochantin, anterior to the insertion site of **IIIdvm2**. It only presents in Psocodea (Fig. 2C) among the paraneopteran taxa examined.

IIIpcm2 is a thick muscle originating from the middle of the basalare and inserting into the lateral metacoxal rim. It is absent in Thysanoptera (Fig. 3) and Sternorrhyncha (Hemiptera) (Fig. 4). This muscle is usually long (Figs 1B and 2B) but is short in Heteroptera (Fig. 5C).

IIIpcm3 runs parallel to **IIIpcm2**, and their distinction is obscure, especially when one of these muscles is absent (see Materials and Methods). It is about the same size with **IIIpcm2** but is tapering dorsally. This muscle originates from the basalare, posterior to the origination site of **IIIpcm2**, and inserts into the metacoxal rim, posterior to the insertion position of **IIIpcm2**. It is absent in Condylgnatha (Figs 3–5).

IIIpcm4 is a muscle originating from the dorsal region of the epimeron and inserting into the lateral coxal rim. It is very long and thin in Psocodea (Fig. 2C) but is very thick and tapering ventrally in Thysanoptera (Fig. 3B). This muscle is absent in Hemiptera (Figs 4–5).

IIIpcm5 is a thick and long muscle originating from the anterior part of the basalare, anterior to the origination site of **IIIpcm2**, and inserting into trochanter via a tendon. It consists of two bundles but is absent in Thysanoptera (Fig. 3) and Heteroptera

(Fig. 5).

IIIpcm6 is a large muscle, consisting of two bundles, observed only in Heteroptera (Fig. 5B) among the taxa examined in this study. It originates from the posterior part of the episternum and inserts into the trochanter via a tendon.

IIIpcm7 is a short muscle originating from the anteroventral edge of the episternum and inserting into the posterior mesocoxal rim. It only presents in Troctomorpha and Psocomorpha (Psocodea: Kawata et al., 2022) among the species examined here.

3.2.4 | Sternal Muscles

IIIvlm2 is a muscle originating from the posterior part of the metafurca and inserted to the abdominal segment. It is absent in Psocodea.

IIIscm1 is a small muscle originating from the posterolateral surface of the furca and inserting into the anterior coxal rim. It sometimes consists of two bundles, as observed in Thysanoptera (Fig. 3D) and Sternorrhyncha (Fig. 4E). This muscle is absent in Psocodea (Fig. 2D).

IIIscm2 is a rather large muscle (among the scm muscles) originating from the posterolateral surface of the furca, posterior to the origination point of **IIIidvm8**, and inserting into the posterior metacoxal rim. This muscle consists of two (Heteroptera: Fig 5E) or three (Psocodea: Fig. 2D; Thysanoptera: Fig. 3D) bundles but is absent in Sternorrhyncha (Hemiptera) (Fig. 4).

IIIscm3 is only observed in Thysanoptera among the paraneopteran taxa examined here (Fig. 3D), originating from the furcal arm, ventral to the origination sites of **IIIscm2** and **6**, and inserting into the mesal coxal rim.

IIIscm4 is only observed in Tubrifera (Thysanoptera) (Online Supplement) among the paraneopteran taxa examined here, originating from the furcal arm, near the origination point of **IIIscm3**, and inserting into the lateral coxal margin.

IIIscm6 is a flat muscle originating from the anteroventral margin of the furcal arm and inserting into the trochanter via a tendon, anterior to the insertion position of **IIIidvm7** (Figs 1–5). It is well developed among the scm muscles and usually consists of multiple bundles.

3.3 | Phylogenetic signal for (non)monophyly of Paraneoptera

When the sister group relationship between Psocodea and Holometabola was

constrained (nonmonophyly of Paraneoptera), as suggested from phylogenomic studies (Misof et al., 2014; Johnson et al., 2018) (other topology were fixed as described in Materials and Methods), tree length (L) was calculated as 158, with consistency index (CI) = 0.42 and retention index (RI) = 0.53. With this topology, no character state supporting Psocodea + Holometabola was recovered (Fig. 6)

When the monophyly of Paraneoptera was constrained, tree scores were improved to be L = 154, CI = 0.43 and RI = 0.55 (Fig. 7). Under this topology, the absence of **IItpm7** (#16: but reversed in Heteroptera), absence of **IIscm3** (#33: also absent in Megaloptera and Lepidoptera and present in Terebrantia), absence of **IIItpm7** (#52: nonhomoplasious, but its absence is also reported from some taxa not examined here: Friedrich & Beutel, 2008), and absence of **IIIspm2** (#59: also absent in Amphiesmenoptera) were recovered as the autapomorphies of Paraneoptera.

In addition, some apomorphies supporting the higher-level phylogeny of paraneopteran taxa were recovered, under the monophyly of Paraneoptera constrained.

A total of eight apomorphies supporting the monophyly of Psocodea were recovered: absence of **IIdivm8** (#9: also absent in Mecoptera and Lepidoptera), absence of **IItpm10** (#18: also absent in Heteroptera and Hymenoptera), absence of **IIscm1** (#31: nonhomoplasious), presence of **IIscm7** (#36: also present in Terebrantia of Thysanoptera), absence of **IIIdivm1** (#39: also absent in Lepidoptera), presence of **IIIpcm4** (#62: also present in Zoraptera, Thysanoptera, and Nannochoristidae), absence of **IIIvlm2** (#66: also absent in Hymenoptera), and absence of **IIIscm1** (#67: also absent in Amphiesmenoptera).

Four apomorphic conditions supporting the monophyly of Condylgnatha were recovered: the absence of **IItpm9** (#17: also absent in Zoraptera and Trichoptera), absence of **IIpcm5** (#28: also absent in Hymenoptera), absence of **IIItpm9** (#53: also absent in Zoraptera and Trichoptera), and absence of **IIIpcm1** (#60: also absent in Zoraptera, Mecoptera and Trichoptera).

A total of nine apomorphies supporting the monophyly of Thysanoptera were recovered: the absence of **IIdivm2/3** (#4: also absent in Hymenoptera), absence of **IIdivm4** (#5: also absent in Hymenoptera), absence of **IIdivm5** (#6: also absent in Hymenoptera and Amphiesmenoptera), absence of **IIpcm2/3** (#26: also absent in Hymenoptera), presence of **IIpcm4** (#27: also present in Zoraptera, Hymenoptera and Nannochoristidae), absence of **IIIdivm7** (#44: also absent in Hymenoptera), absence of **IIItpm1** (#46: nonhomoplasious), presence of **IIItpm4** (#49: also present in Mecoptera), and presence of **IIItpm10** (#54: highly homoplasious).

Three apomorphies supporting the monophyly of Hemiptera were recovered: the absence of **II_{dvm}6** (#7: nonhomoplasious), absence of **II_{scm}4** (#34: also absent in Lepidoptera), and absence of **III_dlm1** (#37: nonhomoplasious).

4 | DISCUSSION

Homology of the muscles

Based on the present observations, homology interpretations proposed for a few muscles of Plecoptera, Thysanoptera, and Megaloptera by Friedrich & Beutel (2008) and those of Psocodea by Kawata et al. (2022) were revised as follows (Fig. 8).

Psocodea: **III_{tpm}1** was overlooked by Kawata et al. (2022) (Fig. 2E). In addition, the psocodean **II/III_{tpm}4** muscle described by Kawata et al. (2022) is homologized here with **II/III_{tpm}5**. The present re-examination revealed that this muscle is inserted into the notal margin (Fig. 2E: agrees with the definition of **II/III_{tpm}5** by Friedrich & Beutel, 2008) rather than the proximal margin of the 1st axillary sclerite (definition of **II/III_{tpm}4** by Friedrich & Beutel, 2008).

Thysanoptera: Mickoleit (1961) observed M.furc.-pl., a thin muscle originating from the tip of the furca and running upwardly, and illustrated it in his figures 26 and 27. This muscle was homologized with **III_{spm}2** by Friedrich & Beutel (2008). We identified a muscle exactly corresponding to the metathoracic M.furc.-pl. as illustrated by Mickoleit (1961: figs 26–27) (Fig. 8B) but confirmed that it is inserted into the coxal rim (Fig. 3CD), not the pleurite. This condition agrees with **III_{scm}3** described by Friedrich & Beutel (2008) rather than **III_{spm}2**. Therefore, we homologized the metathoracic M.furc.-pl. with **III_{scm}3** (Table 2). Note that the mesothoracic **II_{spm}2** exists in Thysanoptera (Fig. 3A), which is homologous to the mesothoracic M.furc.-pl. described by Mickoleit (1961: figs 24, 25).

In addition, Mickoleit (1961) observed two muscles inserting into the trochantin: M.dept.troch.terg. (originating from the tergum and inserting into the trochanteral tendon) and M.depr.troch.pl. (originating from the pleurite and inserting into the trochanteral tendon). According to this description given by Mickoleit (1961), these muscles were homologized by Friedrich & Beutel (2008) as **II/III_{dvm}7** and **III_{pcm}5**, respectively. However, we could not

find such muscles originating from the tergum and inserting into the trochantin, although these muscles are illustrated as large (Mickleit, 1961: figs 24, 26) and are thus less likely to be overlooked. Instead, judging from the illustrations (Mickleit, 1961: figs 24, 26) and the presently scanned images, the size and relative position of *M.depr.troch.terg.* agree completely with those of the posterior bundle of a large dorsoventral muscle identified here as **II/III_{dv}m1** (Fig. 8A). The homology of *M.dept.troch.pl.* is somewhat ambiguous, but its condition, as illustrated in the fig. 26 of Mickleit (1961), also agrees with a part of the **III_{dv}m1** muscle (Fig. 8B). Therefore, we homologized both of them as **II/III_{dv}m1** (Table 2).

The homology of the thysanopteran **II/III_{dv}m1** may also be debatable because this muscle consists of at least two bundles, and the latter one is inserted very close to the coxal margin (Fig. 3A), which may be homologized with **II/III_{dv}m2**. However, in Hemiptera (closest relatives of Thysanoptera), **II/III_{dv}m2** is clearly retained at least in the mesothorax, and the condition of their **II/III_{dv}m1** is very similar to that of thysanopterans (Fig. 4F). Therefore, we homologized both bundles of Thysanoptera as **II/III_{dv}m1**.

Plecoptera: Wittig (1955) observed II/III_{cpm}51 and 52 muscles both originating from the basalare and inserting into the coxal rim. Of them, Friedrich & Beutel (2008) homologized the latter with their **II/III_{pcm}4**. However, **II/III_{pcm}4** is the muscle originating from the pleural arm (Friedrich & Beutel, 2008). In addition, we undoubtedly identified the muscles corresponding to II/III_{cpm}51/52 of Wittig (1955), and our present observation confirmed that these muscles share the same origin/insertion sites (basalare and anterior coxal rim) and are almost inseparable (Online Supplement). Therefore, we concluded that II/III_{cpm}51 and 52 muscles should be identified as two bundles of a single muscle (= **II/III_{pcm}2**), and **II/III_{pcm}4** is missing in Plecoptera (Table 2).

Megaloptera: Maki (1936) observed two muscles inserting into the mesothoracic 3rd axillary sclerite (119a and b). Friedrich & Beutel (2008) identified them as **II_{tpm}8** and **II_{tpm}6**, respectively. However, according to the definition by Friedrich & Beutel (2008), **II_{tpm}6** is the muscle inserting into the notal margin, and **II_{tpm}8** is the muscle inserting into the 2nd axillary sclerite. In the present analyses, we confirmed that the 119ab muscles are

both inserted into the 3rd axillary sclerite (Fig. 1E), as observed by Maki (1936). Therefore, according to the definition by Friedrich & Beutel (2008), the 119a and b muscles are homologized here with **Iitpm9** and **Iitpm7**, respectively (Table 2). In addition, Maki (1936) observed a muscle connecting the subalare and epimeron (120), which was homologized with **Iitpm9** by Friedrich & Beutel (2008). However, this condition agrees with the definition of **Iitpm10** described by Friedrich & Beutel (2008). This muscle condition was also confirmed in the present examination (Fig. 1C).

In addition, some muscles observed in previous studies of Plecoptera, Megaloptera, and Mecoptera were not detected from these orders by the present examinations (Table 2). This may partly represent intraordinal variations, and this is probably the case for the state differences between Nannochoristidae and Panorpidae of Mecoptera (Table 2: data for both were selected from synchrotron μ CT images). However, this may also be due to the size effect, i.e., morphological simplification due to miniaturization. Because of the limitation of the μ CT beam width, relatively to very small-sized species were selected for the present examinations, whereas previous section- or hand-dissection-based observations were based on large species (e.g., small *Nemora* examined here vs. large *Perla* of Plecoptera examined previously). Therefore, such size differences of the sampled specimens may affect the presence/absence of the pterothoracic muscles. In contrast, all the thysanopteran thoracic muscles identified in the previous study could also be confirmed in the present examinations, possibly because both studies were based on minute species. The assumption of simplification according to miniaturization also implies that some of the homoplasies identified in the present analyses could be attributed to the size effect. As shown in Fig. 7 and Table 2, most of the derived thoracic muscle conditions were identified as reductions of small muscles, and most exemplars of each insect order are represented by small species in this study. This can be further tested by examining larger samples in future studies.

A considerable number of homoplasious modifications observed between Thysanoptera and Hymenoptera are notable (Fig. 7). In particular, reductions of some large and highly conserved muscles (such as **Ildvm2/3** and **5**, **Iipcm2/3**, and **IIldvm7**) were exclusively and convergently detected between them. Although the functional aspect of each

muscle is beyond the scope of the present study, Thysanoptera and Hymenoptera could be interesting targets for examining the morphological and functional changes of the thorax, wings and legs and their consequences regarding morphological convergences.

Parsimony character mapping and supporting signal for Paraneoptera

The monophyly of Paraneoptera has long and widely been recognized morphologically, with support from multiple independent character systems (head, wing base, and abdomen: see Introduction). However, based on the fossil evidence, a few morphological characters that had previously been recognized as autapomorphies of Paraneoptera (i.e., reduction of the labial palpi and reduction of the tarsomeres: Beutel et al., 2014) have been recovered to be independently derived between Psocodea and Condylgnatha (Huang et al., 2016; Yoshizawa & Lienhard, 2016). Although the other autapomorphies of Paraneoptera (e.g., elongated lacinia, specialized wing base structures, and reduction of cerci) are also confirmed in the fossil taxa and thus are still valid, some of them are reduction characters and thus are less reliable. Therefore, additional morphological characters are needed to test or validate the phylogenomic results regarding the paraphyly of Paraneoptera. Here, we examined the pterothoracic musculature as a potentially useful character system.

The presence of considerable homoplasies was evident from the distribution of apomorphic condition (Table 2). Therefore, for recovering signals contained in the pterothoracic musculature, we mapped the character matrix on two alternative trees (monophyly of Paraneoptera vs. Psocodea sister to Holometabola). When the sister group relationship between Psocodea and Holometabola was constrained (Fig 6: as recovered phylogenomically), no apomorphic characters supporting their close relationship was recovered (tree length was calculated to be 158). In contrast, when the monophyly of Paraneoptera was constrained (Fig. 7: as suggested morphologically), a total of four apomorphic characters were recovered (tree length = 154). Therefore, the pterothoracic muscles provided additional signal favouring the monophyly of Paraneoptera. However, it should also be noted that all the four apomorphies supporting the monophyly of Paraneoptera are reduction of small muscles and thus are less reliable than gain characters. In addition, two of them are unstable even within Paraneoptera (see Chapter 3.3).

The pterothoracic muscles also provided further support for some higher taxa of Paraneoptera. Although the monophyly of Psocodea has been robustly supported molecularly

and phylogenomically (Yoshizawa & Johnson, 2003; Johnson et al., 2004, 2018; de Moya et al., 2021), morphological support for this order is limited (Beutel et al., 2014). For example, although the wing base morphology provided strong support for the monophyly of Paraneoptera, this character system did not provide any evidence for the monophyly of Psocodea (Yoshizawa & Saigusa, 2001). The present analyses recovered a total of eight pterothoracic muscle apomorphies supporting the monophyly of Psocodea (Fig. 7). The monophyly of Thysanoptera has been consistently supported morphologically, molecularly, and phylogenomically, and the present analyses also recovered many apomorphies for this order (Fig. 7 and Table 2). Monophyly of Hemiptera has also been recognized widely, and clear signals supporting the monophyly of Hemiptera, including two nonhomoplasious apomorphies, were recovered from the pterothoracic musculature (Fig. 7). Some new morphological apomorphies supporting the monophyly of Condylgnatha were also detected, which provides corroborating evidence for the monophyly of Condylgnatha. Again, it should also be noted that almost all the characters are reduction ones, and a small amount of gain characters are highly homoplasious.

In conclusion, although considerable homoplasies exist, and most of detected apomorphies are loss characters, the pterothoracic musculature contains some signals favouring the monophyly of Paraneoptera. More importantly, this character system does not contain any apomorphies supporting Psocodea + Holometabola, the relationship suggested by phylogenomic analyses (Misof et al., 2014; Johnson et al., 2018). Although the systematic value of the pterothoracic musculature identified here is limited, all the morphological data provided to date converged to the monophyly of Paraneoptera (head, wing base, and abdomen, plus thoracic musculature newly added here), including both extant and extinct taxa (Huang et al., 2016; Yoshizawa & Lienhard, 2016; Johnson et al., 2018). Although the phylogenomic studies supported Psocodea + Holometabola with high bootstrap values, monophyly of Paraneoptera as suggested morphologically still remains as a plausible hypothesis (Misof et al., 2014; Johnson et al., 2018).

AUTHOR CONTRIBUTIONS

KY conceived the study. KY and NO collected samples. KY, NO and AK took μ CT images. AK and KY performed 3D reconstructions and interpreted morphology. KY and AK performed parsimonious morphological mapping. AK wrote the first draft in Japanese as his master's thesis, and KY wrote the English manuscript of the paper. All authors read and approved the final manuscript.

ACKNOWLEDGEMENTS

We thank Kentaro Uesugi, Akihisa Takeuchi and Masayuki Uesugi for their technical support in μ CT imaging at SPring-8, and Toshiyuki Oshiki for his support in the field. Research at SPring-8 was approved through project numbers 2016A1269 (Ryuichiro Machida), 2017B1712, 2018B1688, 2018B1725 (NO), 2022A1201 (KY), and 2023A1173 (Yoko Matsumura). This study was partly supported by JSPS Grant 19H03278 to KY and was conducted in part to fulfil a master degree of AK, who thanks Shin-Ichi Akomoto, Masahiro Ôhara, and Yoko Matsumura for their guidances.

CONFLICT OF INTEREST

The authors declare no conflict of interest.

DATA AVAILABILITY STATEMENT

Scanned images and 3D segmentation data compatible for ITK-snap software (free software available for Windows, Mac, and Linux) and NEXUS formatted data matrix analyzed in this study are available as Online Supplement from FigShare at <https://figshare.com/s/1d2dd0451b4f56aae6b2> (private link only for reviewing process: DOI will be provided upon acceptance).

REFERENCES

- Beutel, R. G., Friedrich, F., Hörnschemeyer, T., Pohl, H., Hünefeld, F., Beckmann, F., Meier, R., Misof, B., Whiting, M. F. & Vilhelmsen, L. (2011) Morphological and molecular evidence converge upon a robust phylogeny of the megadiverse Holometabola. *Cladistics* 27: 341–355.
- Beutel, R. G., Friedrich, F., Ge, S. Q. & Yang, X. K. (2014) Insect Morphology and Phylogeny. De Gruyter GmbH.
- Blanke, A., Wipfler, B., Letsch, H., Koch, M., Beckmann, F., Beutel, R. G. & Misof, B. (2012) Revival of Palaeoptera – head characters support a monophyletic origin of Odonata and Ephemeroptera (Insecta) *Cladistics* 28: 560–581.
- Blanke, A., Greve, C., Wipfler, B., Beutel, R. G., Holland, B. R. & Misof, B. (2013) The identification of concerted convergence in insect heads corroborates Palaeoptera. *Systematic Biology* 62: 250–263.
- Brodsky, A. K. (1994) *The Evolution of Insect Flight*. Oxford University Press.

- de Moya, R., Yoshizawa, K., Walden, K. K. O., Sweet, A. D., Dietrich, C. H. & Johnson, K. P. (2021) Phylogenomics of parasitic and non-parasitic lice (Insecta: Psocodea): Combining sequence data and exploring compositional bias solution in next generation datasets. *Systematic Biology* 70: 719–738.
- Friedrich, F. & Beutel, R. G. (2008) The thorax of *Zorotypus* (Hexapoda, Zoraptera) and a new nomenclature for the musculature of Neoptera. *Arthropod Structure & Development* 37: 29–54.
- Friedrich, F. & Beutel, R. G. (2010) The thoracic morphology of *Nannochorista* (Nannochoristidae) and its implication for the phylogeny of Mecoptera and Antiliphora. *Journal of Zoological Systematics and Evolutionary Research* 48: 50–74.
- Hennig, W. (1981) *Insect Phylogeny*. Wiley & Sons.
- Huang, D. Y., Bechly, G., Nel, P., Engel, M. S., Prokop, J. et al. (2016) New fossil insect order Permopsocida elucidates major radiation and evolution of suction feeding in hemimetabolous insects (Hexapoda: Acercaria) *Scientific Reports* 6: 23004.
- Johnson, K. P., Yoshizawa, K. & Smith, V. S. (2004) Multiple origins of parasitism in lice. *Proceedings of the Royal Society of London (B)* 271: 1771–1776.
- Johnson, K. P., Dietrich, C. H., Friedrich, F., Beutel, R. G., Wipfler, B. et al. (2018) Phylogenomics and the evolution of hemipteroid insects. *PNAS* 115: 12775–12780.
- Kawata, A., Ogawa, N. & Yoshizawa, K. (2022) Morphology and phylogenetic significance of the thoracic muscles in Psocodea (Insecta: Paraneoptera). *Journal of Morphology* 283: 1106–1119.
- Kobert, K., Salichos, L., Rokas, A. & Stamatakis, A. (2016) Computing the internode certainty and related measures from partial gene trees. *Molecular Biology and Evolution* 33: 1606–1617.
- Krauss, V., Thümmler, C., Georgi, F., Lehmann, J., Stadler, P. F. & Eisenhardt, C. (2008) Near intron positions are reliable phylogenetic markers: an application to holometabolous insects. *Molecular Biology and Evolution* 25: 821–830.
- Kristensen, N. P. (1991) Phylogeny of extant hexapods. *The Insects of Australia*, pp. 125–140. Melbourne University Press.
- Kumar, S., Filipski, A. J., Battistuzzi, F. U., Kosakovsky Pond, S. L. & Tamura, K. (2012) Statistics and truth in phylogenomics. *Molecular Biology and Evolution* 29: 457–472.
- Machida, R. (2006) Evidence from embryology for reconstructing the relationships of hexapod basal clades. *Arthropod Systematics & Phylogeny* 64: 95–104.
- Maddison, D. R. & Maddison, W. P. (2001) *MacClade 4: Analysis of phylogeny and*

character evolution. Sinauer Inc.

- Maddison, W. P. & Maddison, D. R. (2023) *Mesquite: A modular system for evolutionary analysis, version 3.81*. Available from internet at <https://www.mesquiteproject.org>.
- Maki, T. (1936) Studies of the skeletal structure, musculature and nervous system of the alder fly *Chauliodes formosanus* Petersen. *Memoires of the Faculty of Science and Agriculture, Taihoku Imperial University* 16: 117–243 + 10 plates.
- Maki, T. (1938) Studies on the thoracic musculature of insects. *Memoirs of the Faculty of Science and Agriculture, Taihoku Imperial University* 24: 1–343 + 11 plates.
- Martynov, A. V. (1925) Über zwei Grundtypen der Flügel bei den Insekten und ihre Evolution. *Zeitschrift für Morphologie und Ökologie der Tiere* 4: 465–501.
- Mashimo, Y., Beutel, R. G., Dallai, R., Lee, C. Y. & Machida, R. (2014) Embryonic development of Zoraptera with special reference to external morphology, and its phylogenetic implications (Insecta) *Journal of Morphology* 275: 295–312.
- Matsumura, Y., Wipfler, B., Pohl, H., Dallai, R., Machida, R., Mashimo, Y., Câmara, J. T., Rafael, J. A. & Beutel, R. G. (2015) Cephalic anatomy of *Zorotypus weidneri* New, 1978: new evidence for a placement of Zoraptera. *Arthropod Systematics & Phylogeny* 73: 85–105.
- Mickoleit, G. (1961) Zur Thoraxmorphologie der Thysanoptera. *Zoologische Jahrbücher Abteilung für Anatomie und Ontogenie der Tiere* 79: 1–92.
- Misof, B., Liu, S., Meusemann, K., Peters, R. S., Donath, A. et al. (2014) Phylogenomics resolves the timing and pattern of insect evolution. *Science* 346: 763–767.
- Montagna, M., Tong, K. J., Magoga, G., Strada, L., Tintori, A. et al. (2019) Recalibration of the insect evolutionary time scale using Monte San Giorgio fossils suggests survival of key lineages through the End-Permian Extinction. *Proceedings of the Royal Society, B* 286: 20191854.
- Niehuis, O., Hartig, G., Grath, S., Pohl, H., Lehmann, J., Tafer, H., Donath, A., Krauss, V., Eisenhardt, C., Hertel, J., Petersen, M., Mayer, C., Meusemann, K., Peters, R. S., Stadler, P. F., Beutel, R. G., Bornberg-Bauer, E., McKenna, D. D. & Misof, B. (2012) Genomic and morphological evidence converge to resolve the enigma of Strepsiptera. *Current Biology* 22: 1309–1313.
- Ogawa, N. & Yoshizawa, K. (2017) Morphological dissection of behavior: thoracic musculature clarifies independent development of jumping mechanisms between sister

- groups, planthoppers and leafhoppers (Insecta: Hemiptera: Auchenorrhyncha). *Organisms Diversity & Evolution* 17: 521–530.
- Ribak, G., Dafni, E. & Gerling, D. (2016) Whiteflies stabilize their take-off with closed wings. *Journal of Experimental Biology* 219: 1639–1648.
- Salichos, L. & Rokas, A. (2013) Inferring ancient divergences requires genes with strong phylogenetic signals. *Nature* 497: 327–331.
- Schuh, R. T. & Slater, J. A. (1995) *True Bugs of the World (Hemiptera: Heteroptera)*. Cornell University Press.
- Shen, X. X., Hittinger, C. T. & Rokas, A. (2017) Contentious relationships in phylogenomic studies can be driven by a handful of genes. *Nature Ecology and Evolution* 1: 126.
- Simon, S., Blanke, A. & Meusemann, K. (2018) Reanalyzing the Palaeoptera problem – The origin of insect flight remains obscure. *Arthropod Structure & Development* 47: 328–338.
- Snodgrass, R. E. (1935) *Principles of Insect Morphology*. Cornell University Press.
- Strimmer, K. & von Haeseler, A. (1997) Likelihood-mapping: A simple method to visualize phylogenetic content of a sequence alignment. *PNAS* 94: 6815–6819.
- Swofford, D. L. (2002) *PAUP*: Phylogenetic Analysis Using Parsimony (*and other methods), version 4.0a*. Sinauer Inc.
- Uesugi, K., Hoshino, M., Takeuchi, A., Suzuki, Y. & Yagi, N. (2012) Development of fast and high throughput tomography using CMOS image detector at SPring-8. *Developments in X-Ray Tomography VIII*, Proc SPIE 8506: 850601.
- Uesugi, K., Hoshino, M. & Takeuchi, A. (2017) Introducing high efficiency image detector to X-ray imaging tomography. *Journal of Physics: Conference Series* 849: 012051.
- Wang, Y. H., Engel, M. S., Rafael, J. A., Wu, H. Y., Rédei, D., Xie, Q., Wang, G., Liu, X. G. & Bu, W. J. (2016) Fossil record of stem groups employed in evaluating the chronogram of insects (Arthropoda: Hexapoda). *Scientific Reports* 6: 38939.
- Wipfler, B., Letsch, H., Frandsen, P. B., Kapli, P., Mayer, C. et al. (2019) Evolutionary history of Polyneoptera and its implications for our understanding of early winged insects. *PNAS* 116: 3024–3029.
- Wittig, G. (1955) Untersuchungen am Thorax von *Perla abdominalis* Burm. (Larve und Imago). *Zoologische Jahrbücher Abteilung für Anatomie und Ontogenie der Tiere* 74: 491–570.
- Yoshizawa, K. (2011) Monophyletic Polynoptera recovered by wing base structure. *Systematic Entomology* 36: 377–394.

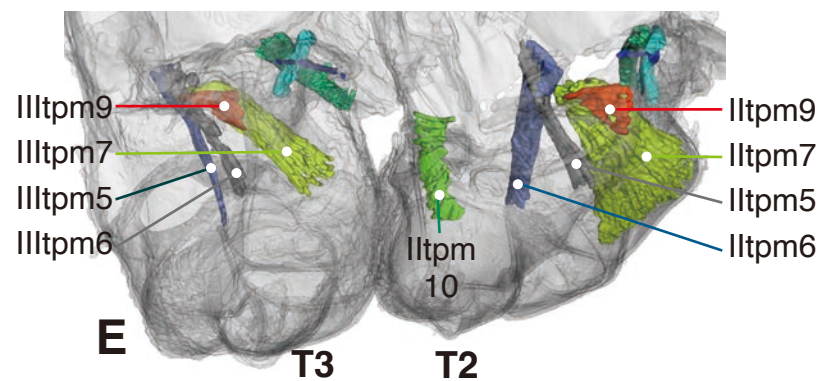
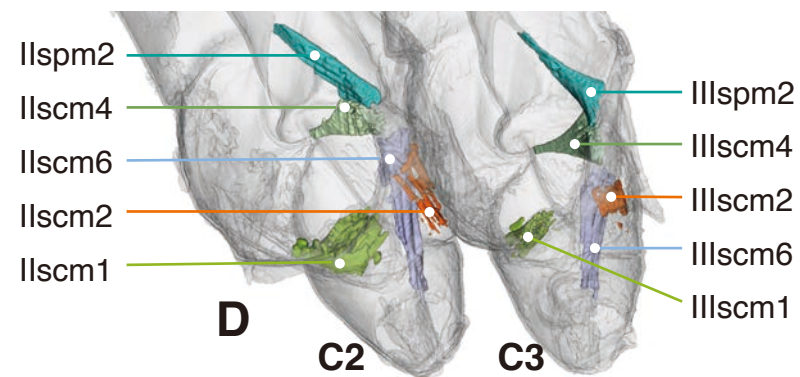
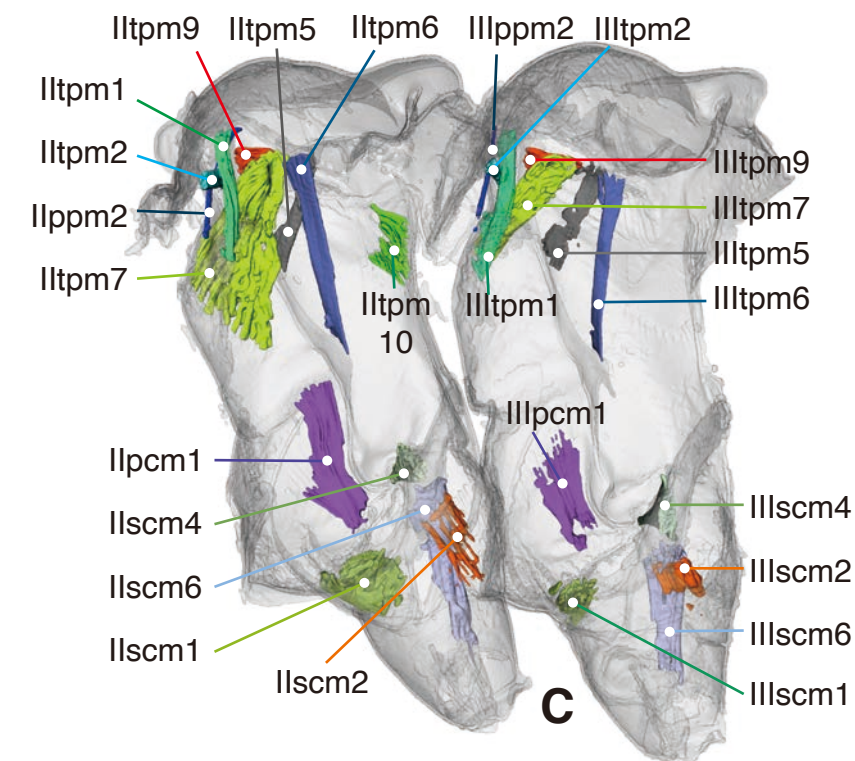
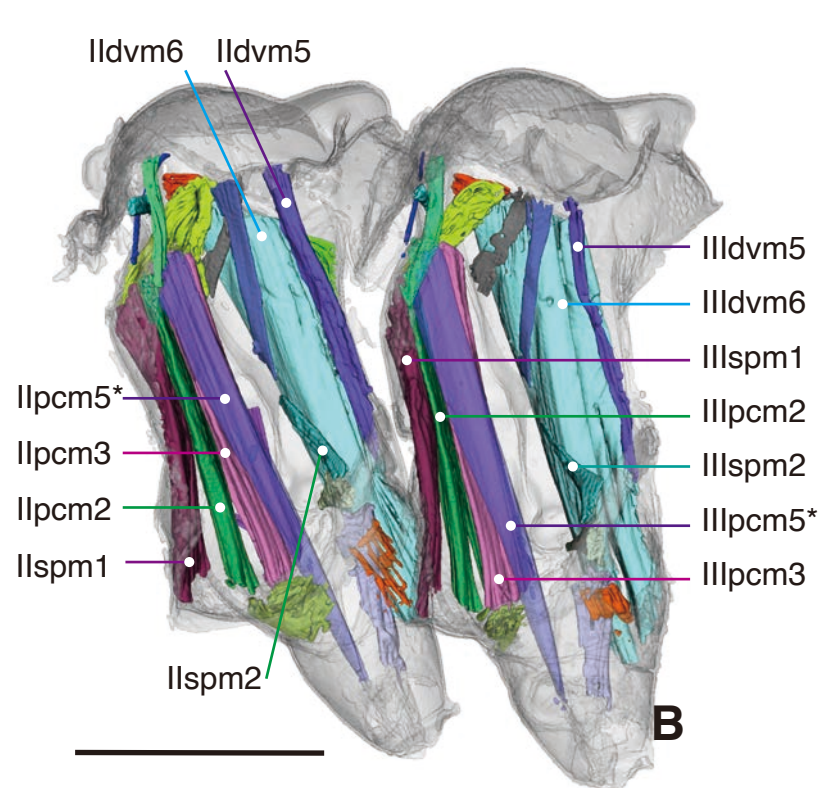
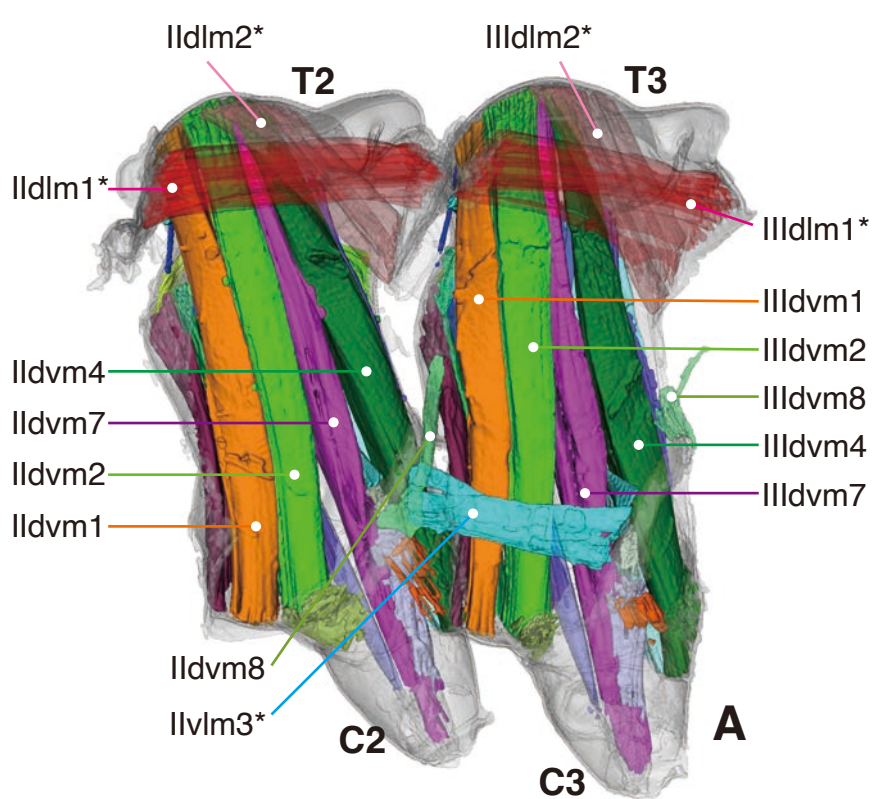
- Yoshizawa, K. & Johnson, K. P. (2003) Phylogenetic position of Phthiraptera (Insecta: Paraneoptera) and elevated rate of evolution in mitochondrial 12S and 16S rDNA. *Molecular Phylogenetics and Evolution* 29: 102–114.
- Yoshizawa, K. & Lienhard, C. (2016) Bridging the gap between chewing and sucking in the hemipteroid insects: new insight from Cretaceous amber. *Zootaxa* 4079: 229–245.
- Yoshizawa, K. & Saigusa, T. (2001) Phylogenetic analysis of paraneopteran orders (Insecta: Neoptera) based on forewing base structure, with comments on monophyly of Auchenorrhyncha. *Systematic Entomology* 26: 1–13.
- Yushkevich, P. A., Piven, J., Hazelett, H. C., Smith, R. G., Ho, S., Gee, J. C. & Gerig, G. (2006) User-guided 3D active contour segmentation of anatomical structures: Significantly improved efficiency and reliability. *NeuroImage* 31: 1116–1128.

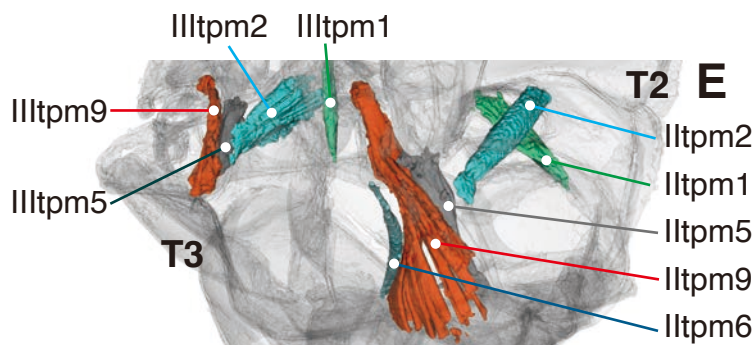
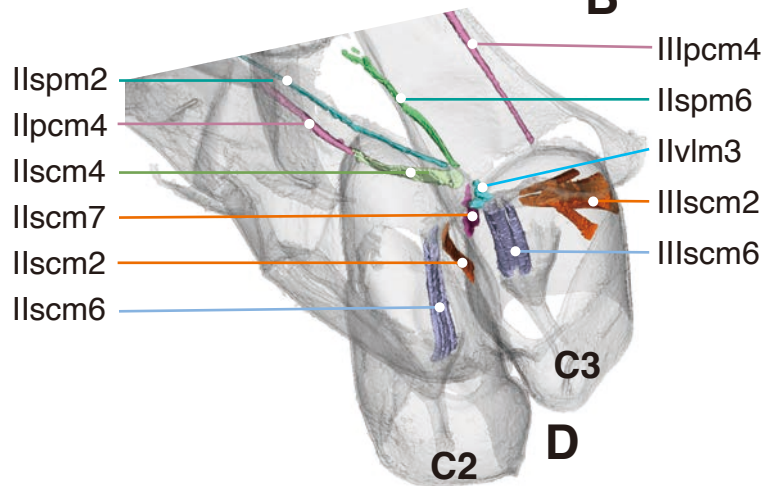
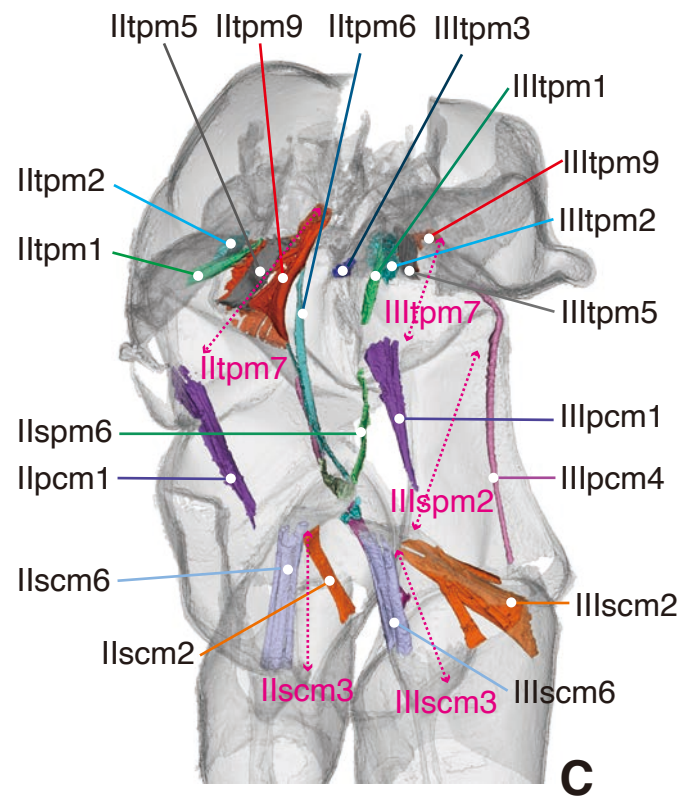
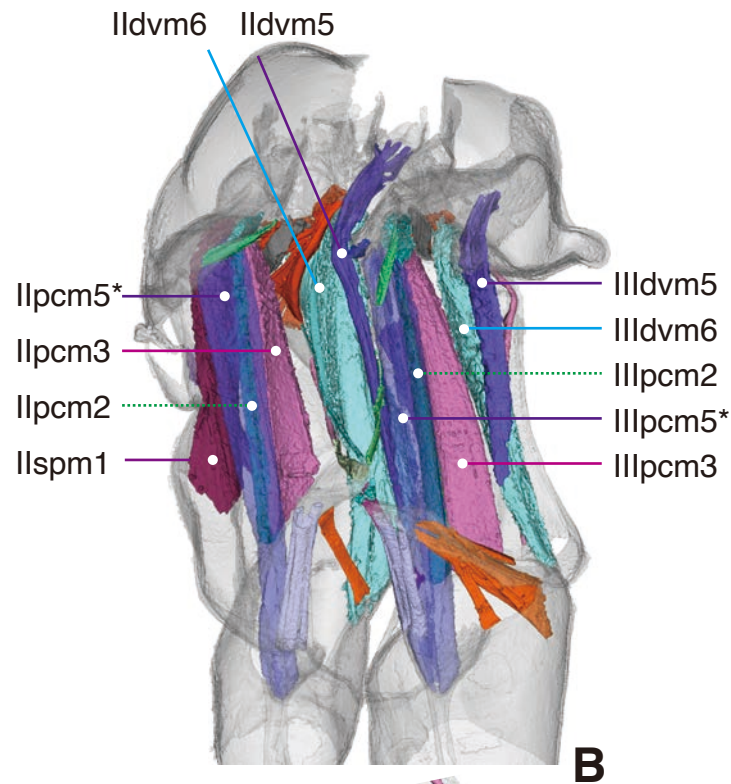
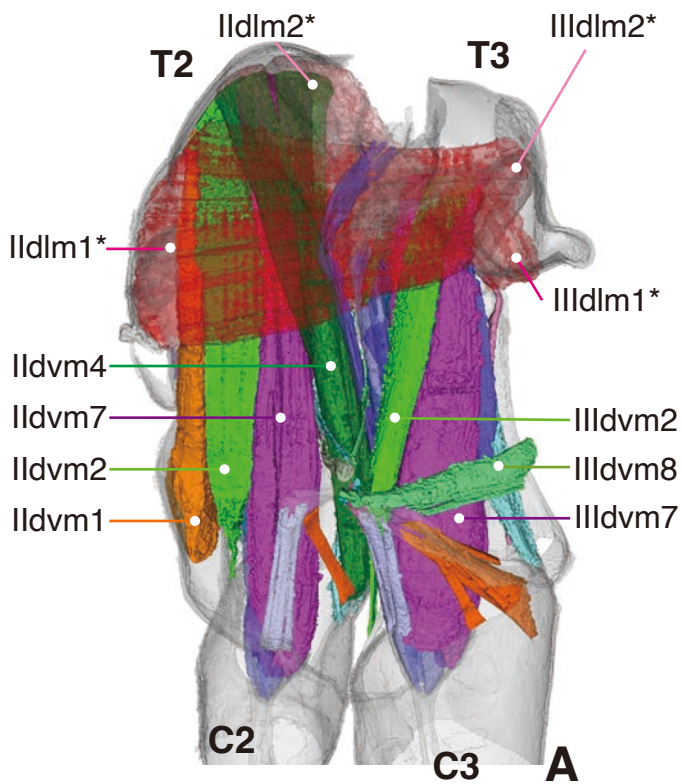
Figure and Table Captions

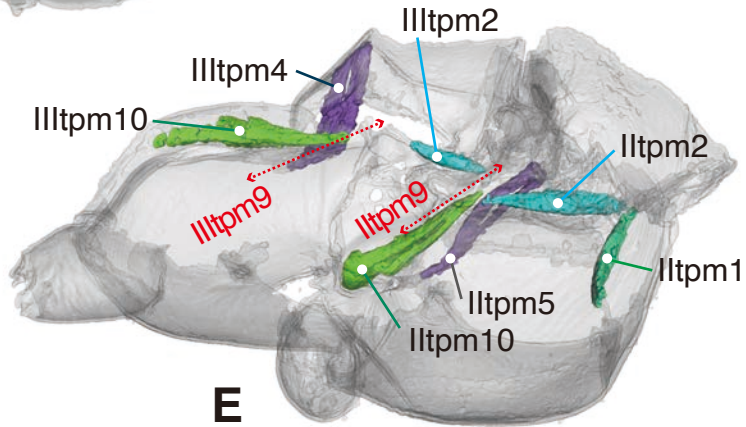
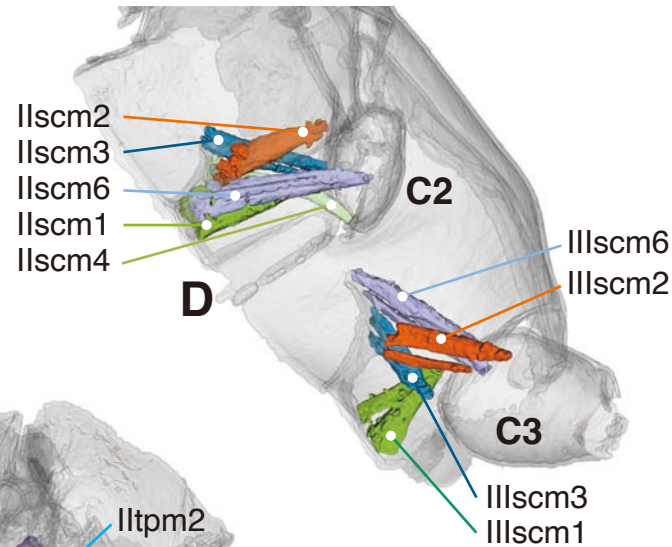
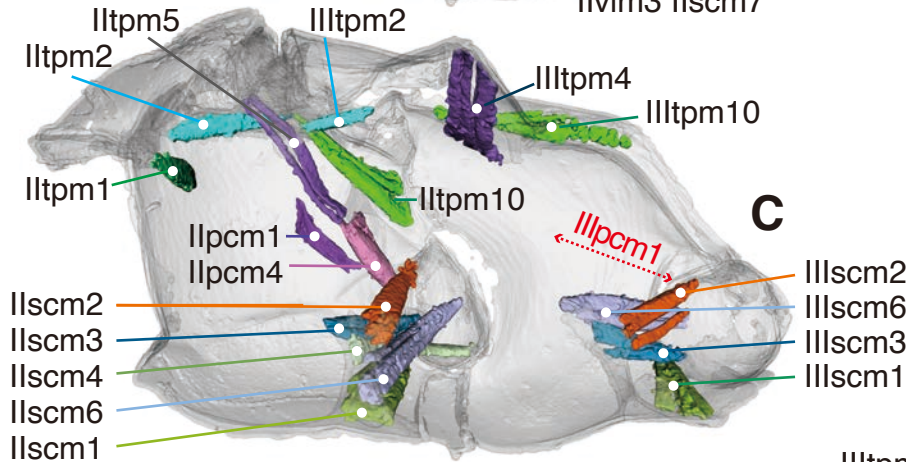
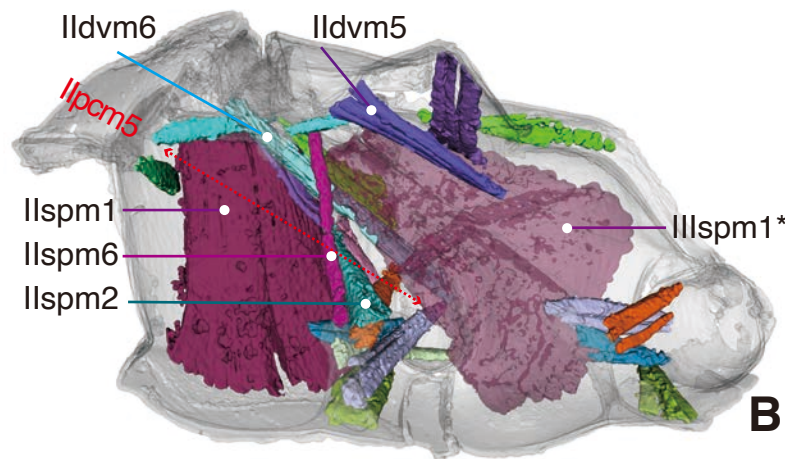
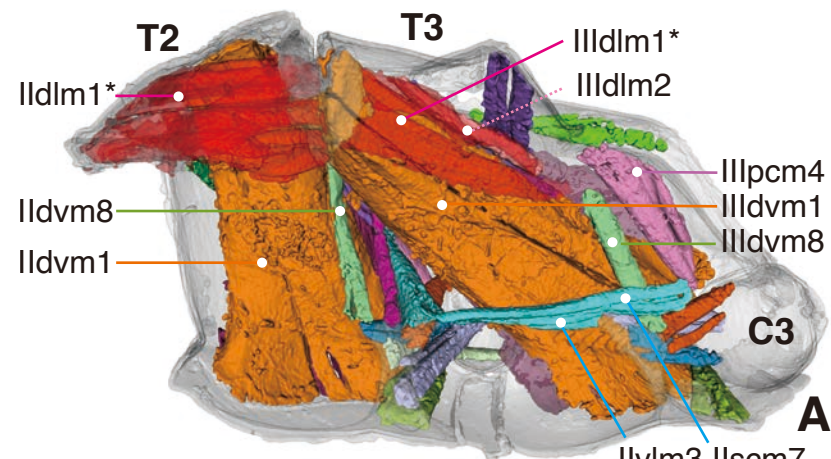
- Fig. 1. 3D reconstruction of the thoracic musculature in Megaloptera. Some muscles indicated by an asterisk (e.g., Ildlm1*) as well as the sclerites are shown as translucent. See text for the muscle names. T2, T3, meso- and metathorax; C2, C3, meso- and metacoxa; PNWP, posterior notal wing process. (A–C) internal view; (D) anterointernal view; (E) dorsolateral view. Scale = 5.0 mm.
- Fig. 2. 3D reconstruction of the thoracic musculature in Trogiomorpha (Psocodea). (A–C) internal view; (D) anterointernal view; (E) dorsolateral view. See Fig. 1 for abbreviations. Scale = 0.1 mm. Red dotted arrows and muscle names indicate missing muscles identified as Paraneopteran autapomorphies.
- Fig. 3. 3D reconstruction of the thoracic musculature in Terebrantia (Thysanoptera). (A–C) internal view; (D) posterointernal view; (E) dorsolateral view. See Fig. 1 for abbreviations. Scale = 0.1 mm. Red dotted arrows and muscle names indicate missing muscles identified as Condylgnathan autapomorphies.
- Fig. 4. 3D reconstruction of the thoracic musculature in Sternorrhyncha (Hemiptera). (A–C) internal view; (D) dorsolateral view; (E, F) posterointernal view. See Fig. 1 for abbreviations. Scale = 0.1 mm. Red dotted arrows and muscle names indicate missing muscles identified as Condylgnathan autapomorphies.
- Fig. 5. 3D reconstruction of the thoracic musculature in Heteroptera (Hemiptera). (A–C) Internal view; (D) dorsolateral view; (E) posterointernal view. See Fig. 1 for abbreviations. Scale = 0.1 mm. Red dotted arrows and muscle names indicate missing muscles identified as Condylgnathan autapomorphies.
- Fig. 6. Parsimonious character mapping on the phylogenomically suggested topology (sister group relationship between Psocodea and Holometabola). Order names are abbreviated as follows: Pso = Psocoptera; Thy = Thysanoptera; Hem = Hemiptera; Mec = Mecoptera. Red squares (nonhomoplasious) and blue triangles (homoplasious, position of homoplasious changes are pointed by the triangle) on the branches indicate apomorphies identified for the clade, and associated numbers indicate character ID: state (absent 0, present 1).
- Fig. 7. Parsimonious character mapping on the morphologically supported topology (monophyly of Paraneoptera). See Fig. 6 for abbreviations and character information.
- Fig. 8. Scanned section images of the metathorax of Terebrantia (Thysanoptera). (A) Anterior region; (B) posterior region. See text for muscle names. Scale = 0.05 mm.
- Table 1. Taxa examined for this study. Subordinal names are given only for the paraneopteran

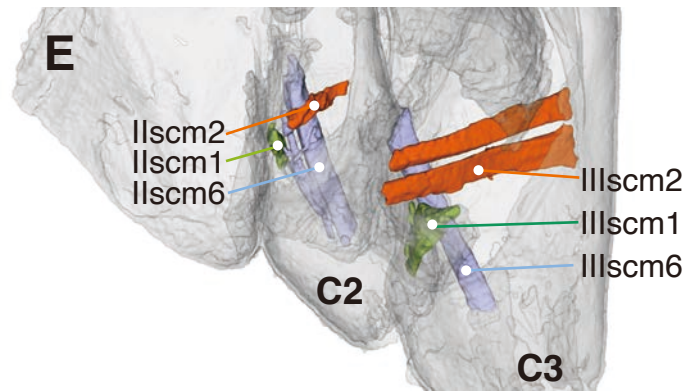
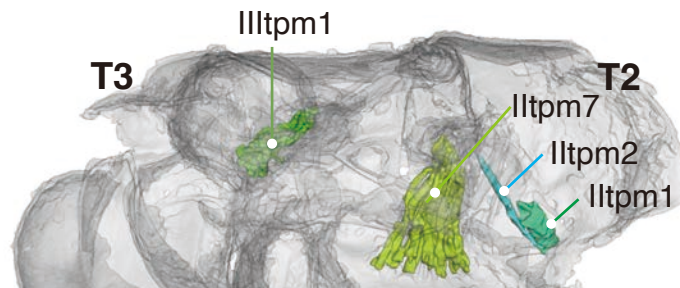
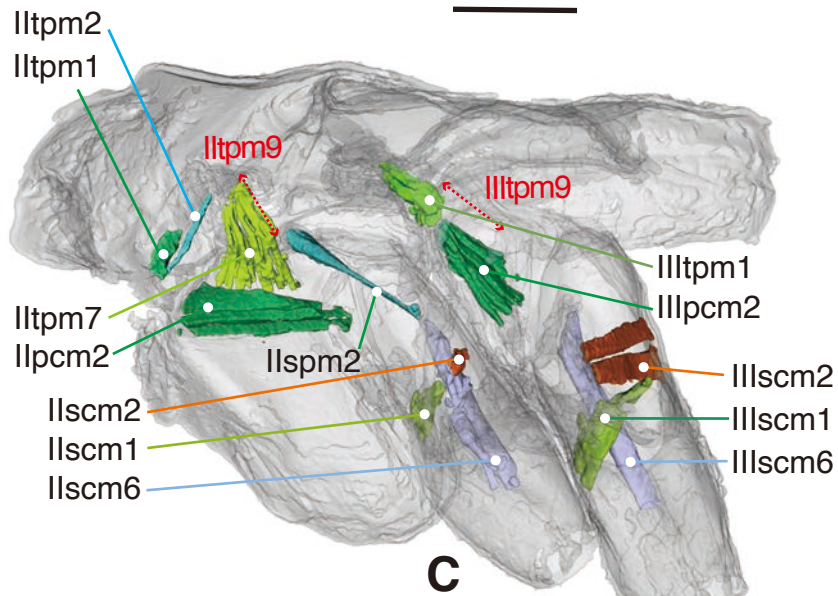
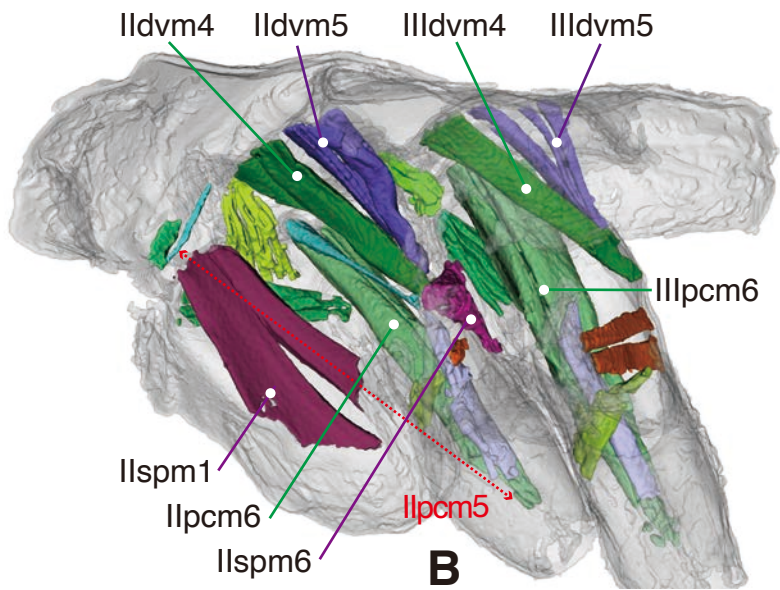
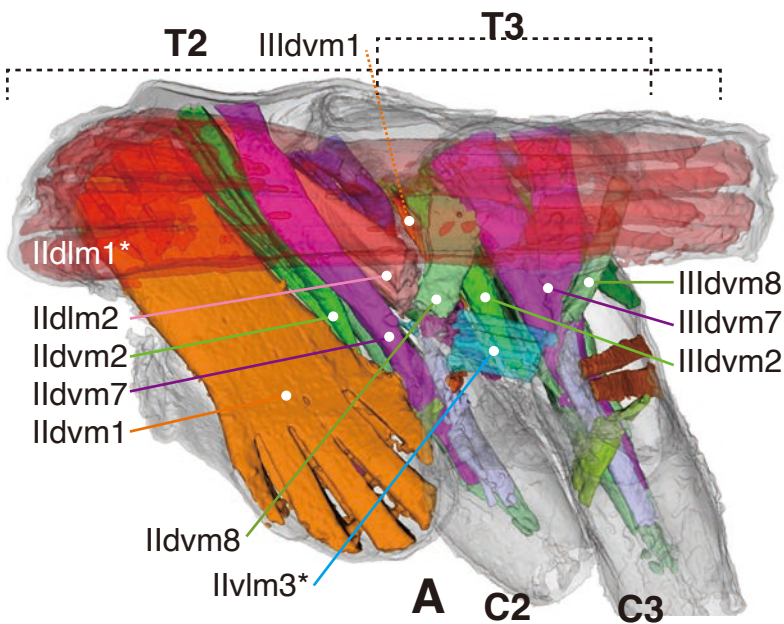
taxa. Resolution of μ CT scan is given in $\mu\text{m}/\text{pixel}$.

Table 2. Presence (1)/absence (0) of each muscle throughout the taxa examined (indicated under Pr.), with their corresponding relations with those of previous studies. The character number (Char#) corresponds to that on the phylogenetic trees (Figs 6–7). Abbreviations are as follows (-ptera was omitted from some ordinal names not mentioned here): Het. – Heteroptera; Psoc. – Psocomorpha; Ste – Sternorrhyncha; Ter – Terebrantia; Troc – Troctomorpha; Trog – Trogiomorpha; F&B – Friedrich & Beutel.

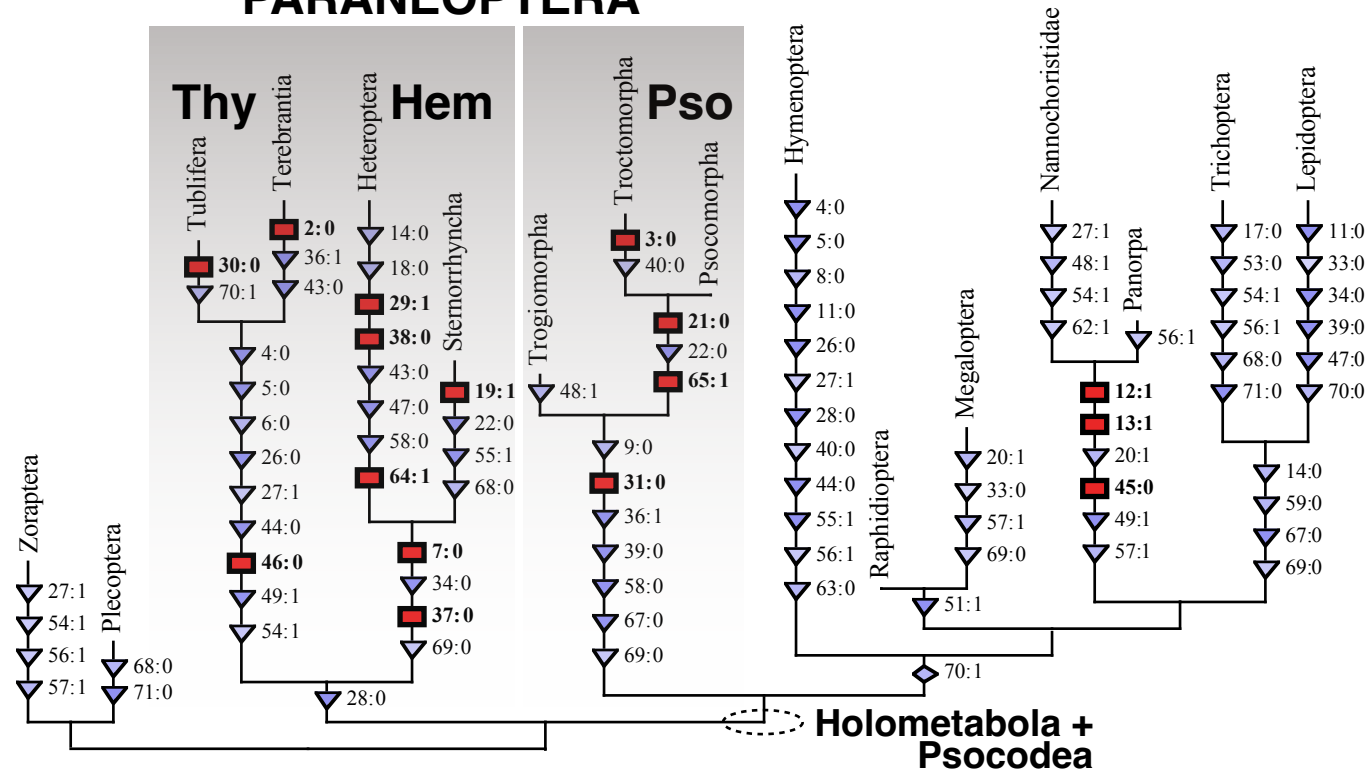




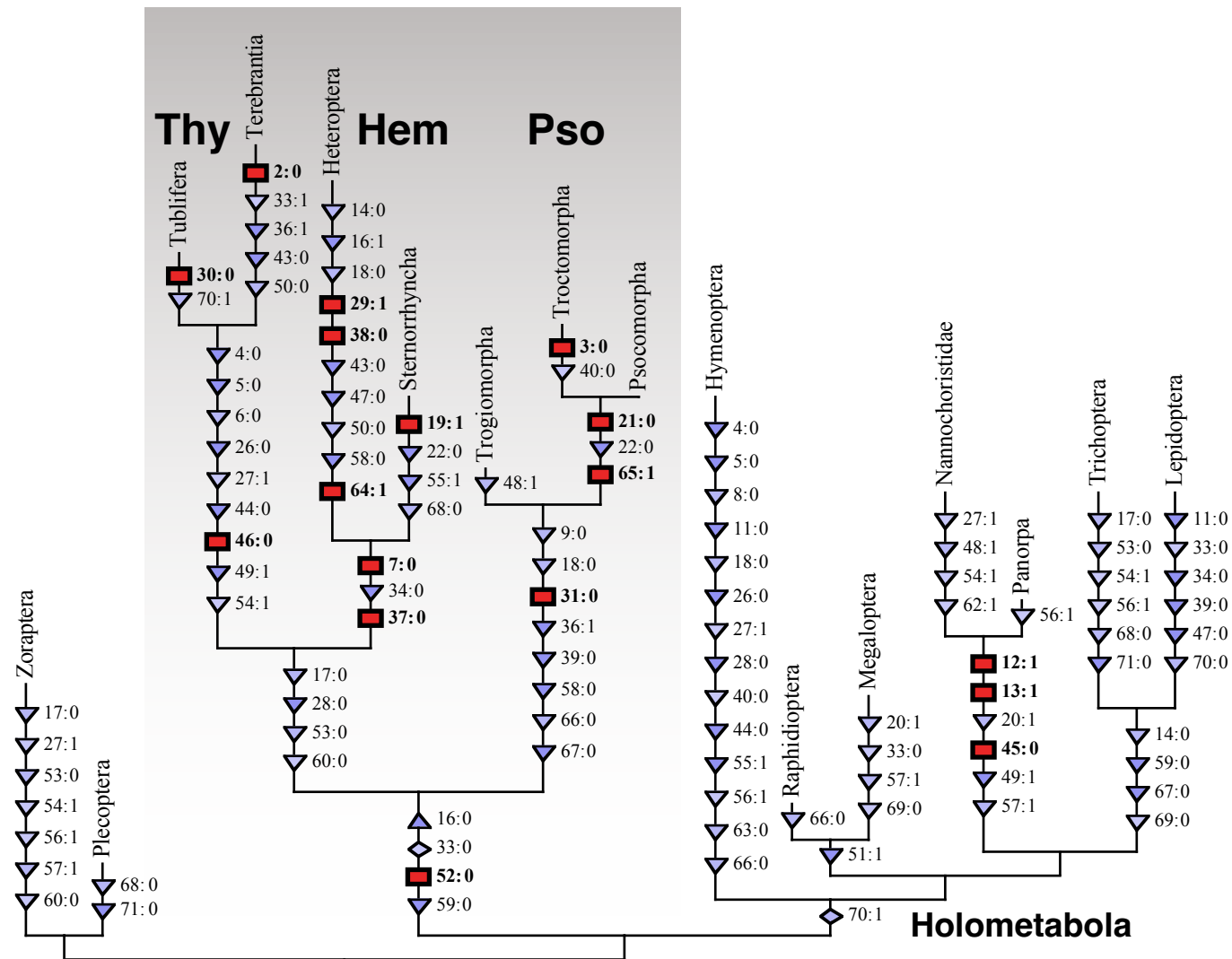


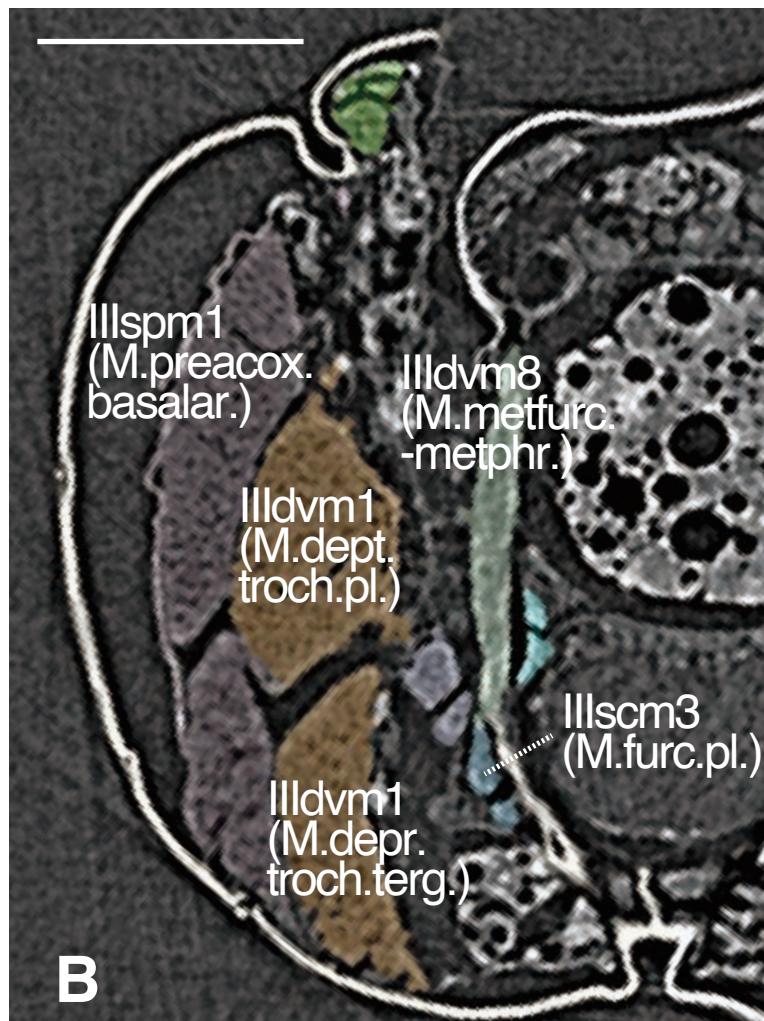
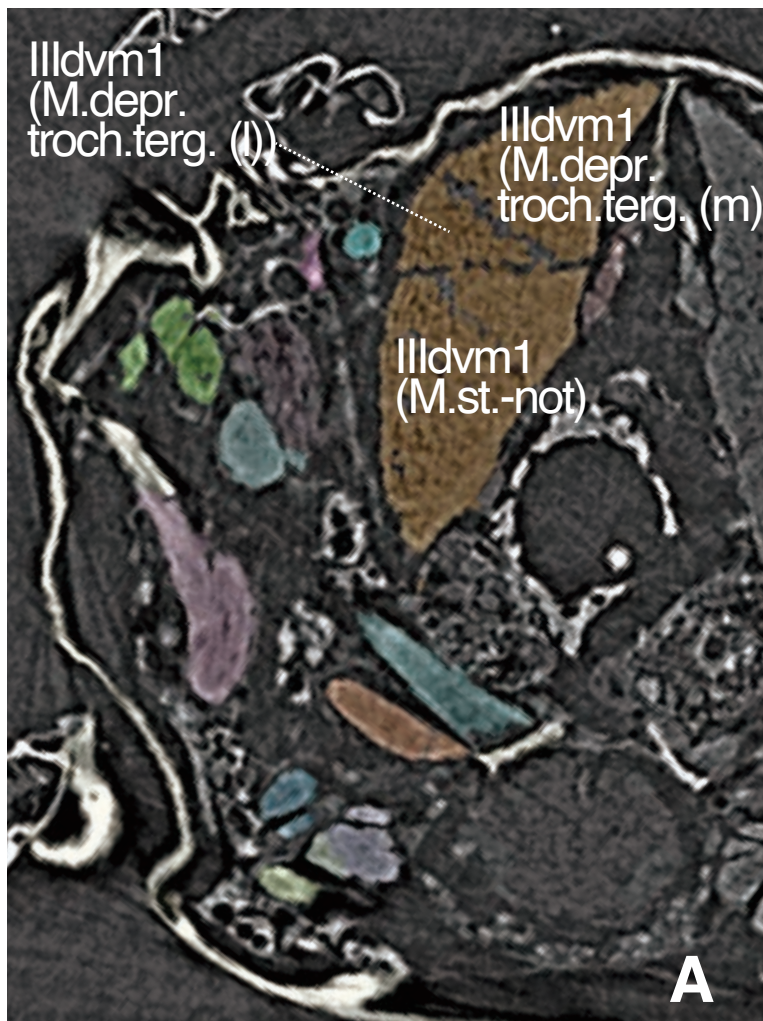


PARANEOPTERA



PARANEOPTERA





Superorder	Order	Suborder	Family	Species	Specimen ID	Locality	resolution
Polyneoptera	Plecoptera		Nemouridae	<i>Nemoura</i> sp.	22KY42	Honshu, Japan	0.85
	Zoraptera		Zorotipidae	<i>Zoroxyptus weidneri</i>	Friedrich & Beutel (2008)		
Paraneoptera	Psocodea	Trogiomorpha	Prionoglarididae	<i>Prionoglaris stygia</i>	Kawata et al. (2022)		
		Troctomorpha	Amphientomidae	Genus sp.	Kawata et al. (2022)		
		Psocomorpha	Caeciliusidae	<i>Valenzuela badiostigma</i>	Kawata et al. (2022)		
	Thysanoptera	Terebrantia	Aeolothripidae	<i>Aeolothrips kurosawai</i>	S8ON07	Hokkaido, Japan	0.49
		Tublifera	Phlaeothripidae	<i>Bactrothrips</i> sp.	23KY01	Honshu, Japan	2.32
	Hemiptera	Sternorrhyncha	Aleyrodidae	<i>Trialeurodes vaporariorum</i>	S8ON14	Hokkaido, Japan	0.49
		Heteroptera	Dipsocoridae	Genus sp.	17ON14	Iriomote, Japan	0.49
Holometabola	Hymenoptera		Tenthredinidae	<i>Aglaostigma sapporonis</i>	22KY05	Hokkaido, Japan	0.85
	Raphidioptera		Inocelliidae	<i>Inocella</i> sp.	22KY07	Hokkaido, Japan	0.85
	Megaloptera		Sialidae	<i>Sialis</i> sp.	S8ON25	Hokkaido, Japan	2.32
	Mecoptera		Panorpidae	<i>Panorpa japonica</i>	22KY08	Honshu, Japan	0.85
			Nannochoristidae	<i>Nannochorista dipteroides</i>	Friedrich & Beutel (2010)		
	Trichoptera		Goeridae	<i>Goera japonica</i>	22KY10	Honshu, Japan	0.85
	Lepidoptera		Adelidae	<i>Nemophora aurifera</i>	22KY30	Hokkaido, Japan	0.85

Char#	Order	Plecoptera		Zora.	Psocodea			Thysanoptera				Hemi.		Hymeno.	Raphidio.	Megalo.		Meco.		Tricho.	Lepido.
	Subord.	Wittig (1955)	Pr.	F&B (2008)	Trog.	Troc.	Psoc.	Tublifera		Tere.	Het.	Ster.	Pr.	Pr.	Maki (1936)	Pr.	F&B (2010)	Pr.	Pr.	Pr.	
	Source				Pr.	Pr.	Pr.	Mickoleit (1961)	Pr.	Pr.	Pr.	Pr.	Pr.	Pr.							
1	Ildm1	Ildm35	1	1	1	1	1	M.dors.rect.	1	1	1	1	1	1	102,103,104	1	1	1	1	1	
2	Ildm2	Ildm36/37	1	1	1	1	1	-	1	0	1	1	1	1	105,106	1	1	1	1	1	
3	Ildvm1	Ildvm40	1	1	1	0	1	M.st-not. M.depr.troch.terg.	1	1	1	1	1	1	112,113	1	1	1	1	1	
4	Ildvm2/3	Ildvm41	1	1	1	1	1	-	0	0	1	1	0	1	127	1	1	1	1	1	
5	Ildvm4	Ildvm43	1	1	1	1	1	-	0	0	1	1	0	1	128,129	1	1	1	1	1	
6	Ildvm5	Ildvm43	1	1	1	1	1	-	0	0	1	1	0	1	130	1	0	0	0	0	
7	Ildvm6	Ildvm53	1	1	1	1	1	M.prom.cox.terg.	1	1	0	0	1	1	136	1	1	1	1	1	
8	Ildvm7	Ildvm42	1	1	1	1	1	-	0	0	1	0	0	1	137	1	1	1	1	1	
9	Ildvm8	Ildvm44	1	1	0	0	0	M.sesphr.-mesfurc.	1	1	1	1	1	1	111	1	0	0	1	0	
10	Iltpm1	Iltpm46a	1	1	1	1	1	M.pl.-terg.epist.caud.	1	1	1	1	1	1	115	1	1	1	1	1	
11	Iltpm2	Iltpm47	1	1	1	1	1	M.pl.-terg.condyl.	1	1	1	1	1	1	116	1	1	1	1	0	
12	Iltpm3	-	0	?	0	0	0	-	0	0	0	0	0	0	-	0	1	1	0	0	
13	Iltpm4	-	0	0	0	0	0	-	0	0	0	0	0	0	117?	0	1	1	0	0	
14	Iltpm5	-	0	0	1	1	1	-	1	1	0	1	1	1	118	1	1	1	0	0	
15	Iltpm6	Iltpm49	1	1	0	0	0	-	0	0	0	0	0	1	-	1	1	1	0	0	
16	Iltpm7	Iltpm48	1	1	0	0	0	-	0	0	1	0	1	1	119b	1	1	1	1	1	
17	Iltpm9	-	1	0	1	1	1	-	0	0	0	0	1	1	119a	1	1	1	0	1	
18	Iltpm10	Iltpm56	1	1	0	0	0	M.pl.-terg.crist.pl.	1	1	0	1	0	1	120	1	1	1	1	1	
19	Iltpm11	-	0	0	0	0	0	-	0	0	0	1	0	0	-	0	0	0	0	0	
20	Iltpm2	Iltpm65/54	1	1	0	0	0	-	0	0	0	0	0	0	107,109	1	1	1	0	0	
21	Iltpm5	Iltpm55	1	1	1	0	0	M.praecox.-basalar.	1	1	1	1	1	1	110	1	1	1	1	1	
22	Iltpm2	Iltzm61a	1	1	1	0	0	M.furc.-pl.	1	1	1	0	1	1	111	1	1	1	1	1	
23	Iltpm4	-	0	0	0	0	0	-	0	0	0	0	0	0	-	0	0	0	0	0	
24	Iltpm6	-	0	0	1	1	1	-	1	1	1	1	1	0	-	0	0	1	1	1	
25	Iltpm1	-	1	0	1	1	1	M.prom.cox.pl.troch.	0	1	0	0	0	1	122	1	0	1	0	1	
26	Iltpm2/3	Iltzm51/52	1	1	1	1	1	-	0	0	1	1	0	1	134,135	1	1	1	1	1	
27	Iltpm4	-	0	1	0	0	0	M.abd.cox.pl.	1	1	0	0	1	0	133	0	1	0	0	0	
28	Iltpm5	Iltzm50	1	1	1	1	1	-	0	0	0	0	0	1	138	1	1	1	1	1	
29	Iltpm6	-	0	0	0	0	0	-	0	0	1	0	0	0	-	0	0	0	0	0	
30	Iltvm3/5	Iltvm38/39	1	1	1	1	1	M.sesfurc.-metfurc.	0	1	1	1	1	1	-	1	1	1	1	1	
31	Iltsm1	Iltzm57	1	1	0	0	0	M.prom.cox.furc.	1	1	1	1	1	1	131	1	1	1	1	1	
32	Iltsm2	Iltzm60	1	1	1	1	1	M.rem.cox.furc.ventr.	1	1	1	1	1	1	132	1	1	1	1	1	
33	Iltsm3	Iltzm59	1	1	0	0	0	-	0	1	0	0	1	1	-	0	1	1	1	0	
34	Iltsm4	Iltzm61b	1	1	1	1	1	M.rem.cox.furc.dors.	1	1	0	0	1	1	126	1	1	1	1	0	
35	Iltsm6	Iltzm58	1	1	1	1	1	M.depr.troch.furc.	1	1	1	1	1	1	139	1	1	1	1	1	
36	Iltsm7	-	0	0	1	1	1	M.mesfurc.metcox.	0	1	0	0	0	0	-	0	0	0	0	0	
37	IIldm1	IIldm35	1	1	1	1	1	M.dors.rect.	1	1	0	0	1	1	152,153,154	1	1	1	1	1	
38	IIldm2	IIldm36/37	1	1	1	1	1	M.metnot.abdterg. M.dors.obl.	1	1	0	1	1	1	155,156	1	1	1	1	1	
39	IIldvm1	IIldvm40	1	1	0	0	0	M.st-not. M.depr.troch.terg. M.depr.troch.pl.?	1	1	1	1	1	1	162,163	1	1	1	1	0	
40	IIldvm2/3	IIldvm41	1	1	1	0	1	-	0	0	1	0	0	1	177	1	1	1	1	1	
41	IIldvm4	IIldvm43	1	1	0	1	1	-	0	0	1	0	0	1	178,179	1	1	1	1	1	
42	IIldvm5	IIldvm43	1	1	1	1	1	M.prom.cox.terg.	1	1	1	1	0	1	180	1	0	0	0	0	
43	IIldvm6	IIlcpm53	1	1	1	1	1	M.cox.-subalar.	1	0	0	1	1	1	186	1	1	1	1	1	
44	IIldvm7	IIlcpm42	1	1	1	1	1	-	0	0	1	1	0	1	187	1	1	1	1	1	
45	IIldvm8	IIlism44	1	1	1	1	1	M.metfurc.-metphr.	1	1	1	1	1	1	161	1	0	0	1	1	
46	IIltpm1	IIltpm46a	1	1	1	1	1	-	0	0	1	1	1	1	164	1	1	1	1	1	
47	IIltpm2	IIltpm47	1	1	1	1	1	M.pl.-terg.condyl.	1	1	0	1	1	1	165	1	1	1	1	0	
48	IIltpm3	IIltpm46b	1	1	1	0	0	-	0	0	0	0	0	0	-	0	1	0	0	0	
49	IIltpm4	-	0	0	0	0	0	M.pl.-terg.crist.pl.	1	1	0	0	0	0	-	0	1	1	0	0	
50	IIltpm5	-	0	0	1	1	1	M.pl.-terg.crist.pl.	1	0	0	1	1	1	167	1	1	1	1	1	
51	IIltpm6	IIltpm49	1	1	0	0	0	-	0	0	0	0	0	1	168	1	0	0	0	0	
52	IIltpm7	IIltpm48	1	1	0	0	0	-	0	0	0	0	1	1	169b	1	1	1	1	1	
53	IIltpm9	-	1	0	1	1	1	-	0	0	0	0	1	1	169a	1	1	1	0	1	
54	IIltpm10	IIlppm56	0	1	0	0	0	-	1	1	0	0	0	0	170	0	1	0	1	0	
55	IIltpm11	-	0	0	0	0	0	-	0	0	0	1	1	0	-	0	0	0	0	0	
56	IIlppm1	IIlism65a	0	1	0	0	0	-	0	0	0	0	1	0	-	0	0	1	1	0	
57	IIlppm2	IIlppm54ab	0	1	0	0	0	-	0	0	0	0	0	0	166	1	1	1	0	0	
58	IIlspm1	IIlspm55	1	1	0	0	0	M.praecox.-basalar.	1	1	0	1	1	1	173,174	1	1	1	1	1	
59	IIlspm2	IIlzm61	1	1	0	0	0	-	0	0	0	0	1	1	175	1	1	1	0	0	
60	IIlpcm1	-	1	0	1	1	1	-	0	0	0	0	1	1	-	1	0	0	0	1	
61	IIlpcm2/3	IIlcpm51/52	1	1	1	1	1	-	0	0	1	0	1	1	185,186	1	1	1	1	1	
62	IIlpcm4	-	0	1	1	1	1	M.abd.cox.pl.	1	1	0	0	0	0	183	0	1	0	0	0	
63	IIlpcm5	IIlcom50	1	1	1	1	1	-	0	0	0	1	0	1	188	1	1	1	1	1	
64	IIlpcm6	-	0	0	0	0	0	-	0	0	1	0	0	0	-	0	0	0	0	0	
65	IIlpcm7	-	0	0	0	1	1	-	0	0	0	0	0	0	-	0	0	0	0	0	
66	IIlvm2	IIlvm64	1	1	0	0	0	M.metfurc.-abdst.	1	1	1	1	0	0	213,215	1	1	1	1	1	
67	IIlsm1	IIlism57	1	1	0	0	0	M.prom.cox.furc.	1	1	1	1	1	1	171	1	1	1	0	0	
68	IIlsm2	IIlism60	0	1	1	1	1	M.rem.cox.furc.ventr.	1	1	1	0	1	1	172	1	1	1	0	1	
69	IIlsm3	IIlism59	1	1	0	0	0	M.furc.-pl.	1	1	0	0	1	1	-	0	1	1	0	0	
70	IIlsm4	-	0	0	0	0	0	M.rem.cox.furc.dors.	1	0	0	0	1	1	176	1	1	1	1	0	
71	IIlsm6	IIlcpm58	0	1	1	1	1	M.depr.troch.furc.	1	1	1	1	1	1	189	1	1	1	0	1	